

170400-3-F

ADA 124277

12

Final Report

# THREE-DIMENSIONAL VISION SYSTEM FOR THE ADAPTIVE SUSPENSION VEHICLE

DAVID M. ZUK and MARK L. DELL'EVA  
Infrared and Optics Division

JANUARY 1983

Approved for Public Release;  
Distribution Unlimited

Sponsored by:

Defense Advanced Research Projects Agency (DoD)

ARPA Order No. 4468

Under Contract No. MDA903-82-C-0119

Issued by:

Department of Army,

Defense Supply Service-Washington,

Washington, D.C. 20310

DTIC  
ELECTE  
FEB 10 1983  
S D E

**Σ ENVIRONMENTAL  
RESEARCH INSTITUTE OF MICHIGAN**

BOX 8618 • ANN ARBOR • MICHIGAN 48107

88 02 010 036

# **NOTICE**

**The views and conclusions contained in this document are those of the authors and should not be interpreted as representing the official policies, either expressed or implied, of the Defense Advanced Research Projects Agency or the U.S. Government.**

---

SECURITY CLASSIFICATION OF THIS PAGE (When Data Entered)

REPORT DOCUMENTATION PAGE		READ INSTRUCTIONS BEFORE COMPLETING FORM
1. REPORT NUMBER 170400-3-F	2. GOVT ACCESSION NO. ADA124 277	3. RECIPIENT'S CATALOG NUMBER
4. TITLE (and Subtitle) THREE-DIMENSIONAL VISION SYSTEM FOR THE ADAPTIVE SUSPENSION VEHICLE		5. TYPE OF REPORT & PERIOD COVERED Final Report
		6. PERFORMING ORG REPORT NUMBER
7. AUTHOR(s) David Zuk and Mark Dell'Eva		8. CONTRACT OR GRANT NUMBER (s) MDA903-82-C-0119
9. PERFORMING ORGANIZATION NAME AND ADDRESS Environmental Research Institute of Michigan P. O. Box 8618 Ann Arbor, Michigan 48107		10. PROGRAM ELEMENT, PROJECT TASK AREA & WORK UNIT NUMBERS
11. CONTROLLING OFFICE NAME AND ADDRESS Defense Advanced Research Projects Agency 1400 Wilson Boulevard Arlington, Virginia 22209		12. REPORT DATE December/1982
		13. NUMBER OF PAGES
14. MONITORING AGENCY NAME AND ADDRESS (if different from Controlling Office) Defense Supply Service-Washington Room 1D-245, The Pentagon Washington, D. C. 20310		15. SECURITY CLASS. (of this report) Unclassified
		15a. DECLASSIFICATION/DOWNGRADING SCHEDULE
16. DISTRIBUTION STATEMENT (of this Report)		
17. DISTRIBUTION STATEMENT (of the abstract entered in Block 20, if different from Report)		
18. SUPPLEMENTARY NOTES		
19. KEY WORDS (Continue on reverse side if necessary and identify by block number) Walking Machine, Three-Dimensional Imaging, Terrain Simulation, Vision Sensor, Adaptive Suspension		
20. ABSTRACT (Continue on reverse side if necessary and identify by block number) This report documents the collection of simulated three-dimensional (3D) terrain data, and the conceptual design of a 3D vision system for the 84 Adaptive Suspension Vehicle (ASV). Descriptions of the 10 scenes on which 3D data was collected are presented along with some samples of 3D data. The results of the conceptual design are included and specifica- tions for the ASV vision mode are presented.		

## THREE-DIMENSIONAL VISION SYSTEM FOR THE ADAPTIVE SUSPENSION VEHICLE

### SUMMARY

This final report documents work of the Environmental Research Institute of Michigan (ERIM) under Defense Advanced Research Projects Agency (DARPA) contract MDA903-82-C-0119, Order Number 4468. The objectives of this contract were to design a three-dimensional (3D) vision system to meet the requirements of the 84 Adaptive Suspension Vehicle (ASV) and to collect data similar to what the proposed system would generate so that the guidance algorithms could be exercised. Two tasks were defined under these objectives: (1) modify the existing Tabletop Three-Dimensional Sensor (T3DS) and collect sample range data on model terrain scenes, and (2) conduct a sensor design study to outline the basic performance parameters and determine methods of hardware implementation.

Task I, scanner modifications, resulted in various optical-mechanical changes, a significant decrease in range noise, and improvement in linearity through the implementation of an improved digital phase detector. Terrain scene models (1/6 scale) were constructed and used with the modified scanner to collect image data for use by other DARPA contractors for algorithm development. As a result of this task, 86 images consisting of 128 x 128 pixels of ten scenes were delivered.

Task II, sensor conceptual design study, involved a general examination of optical and mechanical factors in relation to sensor operating requirements. This examination resulted in the recommendation of a design to achieve the following desired performance: the sensor should have a 1 deg instantaneous field of view (IFOV), a  $\pm 30$  deg total field of view (TFOV), an ambiguity interval of 30 ft (9.14 m), a noise equivalent range of 3 in. (7.6 cm) or less, a frame rate of 2 Hz, a volume of 2 cu ft ( $.056 \text{ m}^3$ ) or less, weigh 50 lbs (23 Kg) or less, and consume less than 1 Kw of electrical power.

# ACKNOWLEDGEMENTS

The authors would like to express their gratitude to the following people without whose assistance this work could not have been performed: Max Bair, Dwayne Carmer, Cindy Conley, John Candlish, Neil Griffin, Tom Griffin, Ed Grigg, Jim Ladd and Vern Larrowe. Furthermore, we thank Dr. Robert McGhee of Ohio State University and Mark Patterson of Battelle for their efforts in working with us in defining the sensor and data collection program.

A special thanks to Dr. Clinton Kelly, III, whose vision of an Adaptive Suspension Vehicle and support from DARPA has made the program possible.

Accession For		
NTIS GRA&I		<input checked="" type="checkbox"/>
DTIC TAB		<input type="checkbox"/>
Unannounced		<input type="checkbox"/>
Justification		
By _____		
Distribution/		
Availability Codes		
Dist	Avail and/or Special	
A		

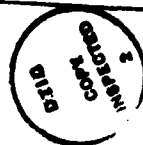


## TABLE OF CONTENTS

	Page
SUMMARY . . . . .	3
LIST OF ILLUSTRATIONS . . . . .	7
LIST OF TABLES . . . . .	9
1 INTRODUCTION . . . . .	11
1.1 3D TECHNOLOGY . . . . .	11
1.2 DATA COLLECTION . . . . .	16
1.3 SYSTEM STUDY . . . . .	17
2 TECHNICAL DISCUSSION . . . . .	19
2.1 TASK I: DATA COLLECTION . . . . .	19
2.1.1 Sensor Improvements	19
2.1.2 Scene Modelling and Data Collection	21
2.2 TASK II: CONCEPTUAL DESIGN . . . . .	55
2.2.1 Wavelength Selection	55
2.2.2 Source and Receiver Optics	60
2.2.3 Scan Mechanism	60
2.2.4 Electronics	65
2.2.5 System Performance	72
2.2.6 ASV Terrain Sensor Parameters	77
3 CONCLUSIONS AND RECOMMENDATIONS . . . . .	79

## LIST OF FIGURES

<u>Figure</u>		<u>Page</u>
1(a)	Range Signal for Laser Scan Line . . . . .	13
1(b)	Range Changes for Two Scan Lines . . . . .	13
2	Block Diagram of 3D Sensor . . . . .	15
3	TFOV Footprint Size on Typical Scene . . . . .	22
4	Semi-Overhead Photo - Slope Module . . . . .	24
5	Semi-Overhead Photo - Trail Module . . . . .	25
6	Semi-Overhead Photo - Cliff Module . . . . .	26
7	Semi-Overhead Photo - Ditch Module . . . . .	27
8	Slope Module . . . . .	28
9	Trail Module . . . . .	29
10	Cliff Module . . . . .	30
11	Ditch Module . . . . .	31
12	Scene 1 Module Configuration . . . . .	35
13	Scene 2 Module Configuration . . . . .	36
14	Scene 3 Module Configuration . . . . .	37
15	Scene 4 Module Configuration . . . . .	38
16	Scene 5 Module Configuration . . . . .	39
17	Scene 6 Module Configuration . . . . .	40
18	Scene 7 Module Configuration . . . . .	41
19	Scene 8 Module Configuration . . . . .	42
20	Scene 9 Module Configuration . . . . .	43
21	Scene 10 Module Configuration . . . . .	44
22	Photograph of Scene 10 Looking in Direction of Scanner Motion. . . . .	46
23	Range Data Image of Scene 10 Footprints 1 Through 4. . . . .	47
24	Photography of Scene 5 Looking in Direction of Scanner Motion . . . . .	49
25	Range Data Image Of Scene 5 Footprints 1 Through 4. . . . .	50

## LIST OF FIGURES (Continued)

<u>Figure</u>		<u>Page</u>
26	Photo of Scene, a Range Image of that Scene and a Line Plot Showing Detail in the Range Data. .	52
27	Sensor Bridge and Scanner Electronics. . . . .	53
28	Scanner Horizontal Position. . . . .	54
29	Position of Ambiguity Interval in Relation to Vertical FOV . . . . .	56
30	Sensor Measurement Reference Point . . . . .	57
31	Laser Collimation Optics . . . . .	61
32	Optical Diagram of Scanner . . . . .	62
33	Drive Requirements for an Oscillating Horizontal Scan Mirror (Torque) . . . . .	64
34	Representation of 60° x 60° Scan System . . . . .	66
35	Scale Representation of 90° x 90° Scan System . . .	67
36	ASV Sensor Field of View . . . . .	68
37	Scan Geometry (Top View 10 ft/sec) . . . . .	69
38	Signal Processing Electronics Block Diagram . . .	70
39	Digital Phase Detector Block Diagram . . . . .	71
40	Range Noise vs Range . . . . .	73
41	Range Noise and S/N vs Receiver Aperture . . . . .	74



## LIST OF TABLES

<u>Table</u>		<u>Page</u>
1	Table Top Scanner Parameters . . . . .	21
2	Approximate Sizes of Scene Surface Materials . . .	32
3	Scene Matrix . . . . .	45
4	Design Goals . . . . .	58
5	Comparison of 0.8 $\mu\text{m}$ and 10.6 $\mu\text{m}$ Sources . . . . .	59
6	Drive Requirements for an Oscillating Horizontal Scan Mirror (Acceleration) . . . . .	63
7	Sensor Parameters . . . . .	78

## SECTION 1

### INTRODUCTION

This introduction consists of three parts. Section 1.1 is a generalized description of a 3D sensor to familiarize the reader with the concept as used in this report. Section 1.2 discusses collection of 3D terrain data. A discussion of the ASV terrain sensor study is in Section 1.3. Details are contained in the technical discussion, Section 2.

#### 1.1 3D TECHNOLOGY

Human mobility and navigation of vehicles are greatly enhanced by the stereo vision provided by our eyes and appropriate data processing in the brain. The essence of stereo vision is the perceived range information that is interpreted as object size, distance, and basic terrain profile. Such information allows a person to select a route and anticipate changes in height or angle of the terrain ahead. The operator of the ASV requires assistance in the evaluation of terrain for the placement of the mechanical feet. If range and profile information could be obtained by an auxiliary sensor and processed by a computer, then the vehicle could move faster and smoother along a better route.

The 3D sensor technology developed at ERIM over the past six years for the Air Force and DARPA offers an excellent alternative to human stereo vision. The sensor employs a scanned laser and generates a true 3D image where distance along the line of sight is either absolute range (R units from the sensor to the object point) or relative range (relative range is the remainder obtained when one performs integral division of the absolute range by the ambiguity

interval). The system proposed for the ASV sensor is a raster scanned or framing imager which provides absolute range data.

The concept behind the ERIM 3D sensor is simply that of an optical radar. A pulse of light is transmitted to the object and returns to the receiver through a process of scattering or reflection by the object's surface. A circuit in the receiver measures the round-trip travel time and produces a signal that we interpret as range,  $R$ ,

where  $R = 1/2 ct$

$c$  = velocity of light =  $9.83 \times 10^8$  ft/sec ( $2.99 \times 10^8$  m/sec)

$t$  = round-trip travel time

If the signal is a voltage that varies between 0 and 1 for ranges between 0 and 32 ft (9.75 m), then the output of 0.5 V means that an object (or the ground) at a 16 ft (4.87 m) range is illuminated. When the laser is scanned along a line, the signal ( $V$ ) as a function of scan angle ( $\theta$ ) could appear as in Figure 1(a). The voltage is higher at the end of the scan line because the range to the Earth increases as  $R_0/\cos\theta$  where  $R_0$  is the range for  $\theta = 0$ ; the arc on the left could be due to a cylindrical tree trunk while the rectangular pattern in the center could be due to a flat object as illustrated in Figure 1(b).

Figure 1(a) illustrates only two dimensions, azimuth scan angle,  $\theta$ , and range,  $R$ . If the laser beam elevation angle is lowered by a small angle,  $\Delta\phi$ , and  $\theta$  is scanned again, the voltage pattern for the Earth will decrease slightly,  $\Delta R_1$  in Figure 1(b) but the tree or flat surface signal will increase slightly,  $\Delta R_2$  in Figure 1(b). Some elevated positions for the sensor are assumed here and Figure 1(b) represents a view for two azimuth lines, one that hits the Earth and another that hits the object. The size of  $\Delta R_1$  or  $\Delta R_2$  depends only on the geometry of the scene. As successive scan lines are obtained by

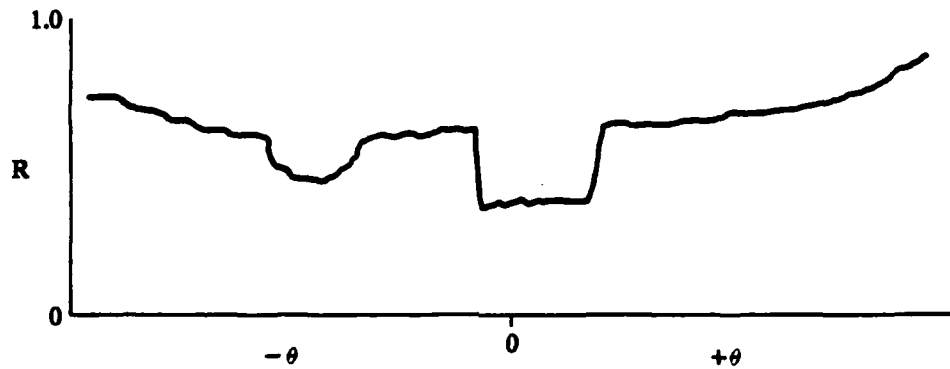


FIGURE 1(a). RANGE SIGNAL FOR LASER SCAN LINE

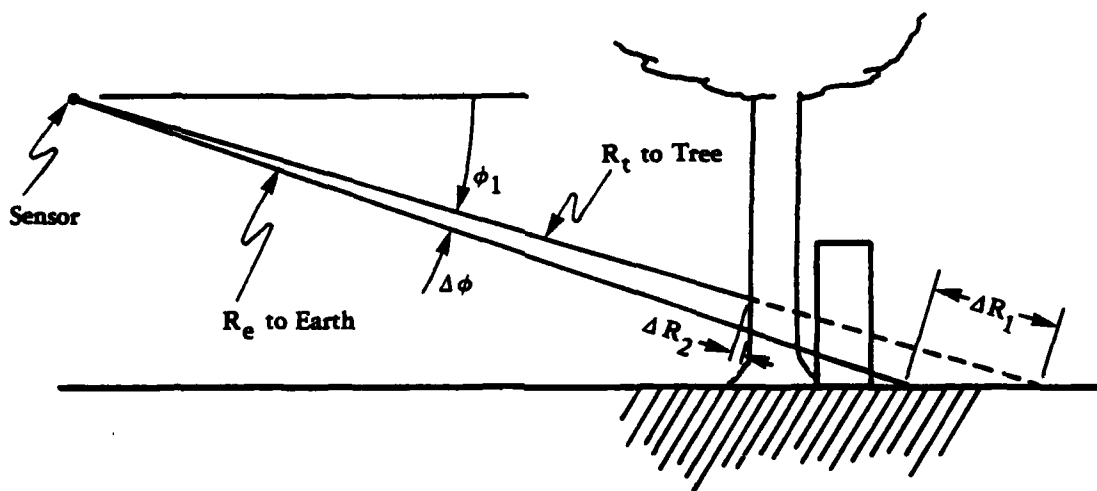


FIGURE 1(b). RANGE CHANGES FOR TWO SCAN LINES

incrementing  $\phi_1$ , one derives the third dimension to complete the location  $\theta$ ,  $\phi$ ,  $R$  for any object or area in the scene. Note that a conventional image gives only  $\theta$  and  $\phi$  information along with intensity.

If one is not interested in the absolute range to the Earth but rather in relative range within or between objects on the Earth, then the transmitter can be pulsed more often so that a whole series of pulses are scattered by the target. Now, the phase of the fundamental Fourier components of the received pulse train is compared with the transmitted pulse train and a voltage is derived that represents the possible 0 to  $2\pi$  phase difference. The range difference that will cause the phase to change by  $2\pi$  is called the ambiguity range,  $R_a$ , and is defined as

$$R_a = \frac{c}{2f}$$

where  $f$  = pulse repetition frequency, and  $c$  = velocity of light. For example, if  $f = 15.36$  MHz, then

$$R_a = \frac{9.83 \times 10^3}{2 \times 15.36 \times 10^6} = 32 \text{ ft} \quad (9.75 \text{ m})$$

With an ambiguity interval of 32 ft (9.75 m), one can measure range up to 32 ft (9.75 m) and then the measurements become ambiguous (i.e., objects at ranges of 1 (0.3 m) or 33 ft (10.05 m) give the same range measurement).

A simplified block diagram of a 3D sensor is presented in Figure 2. The 3D sensor consists of a scanning mechanism which directs the laser beam and field of view of the detector to the scene. The modulation driver provides a modulated light source via the laser and also a phase reference signal to the phase detector. The optical detector converts the modulated optical energy to an electrical signal

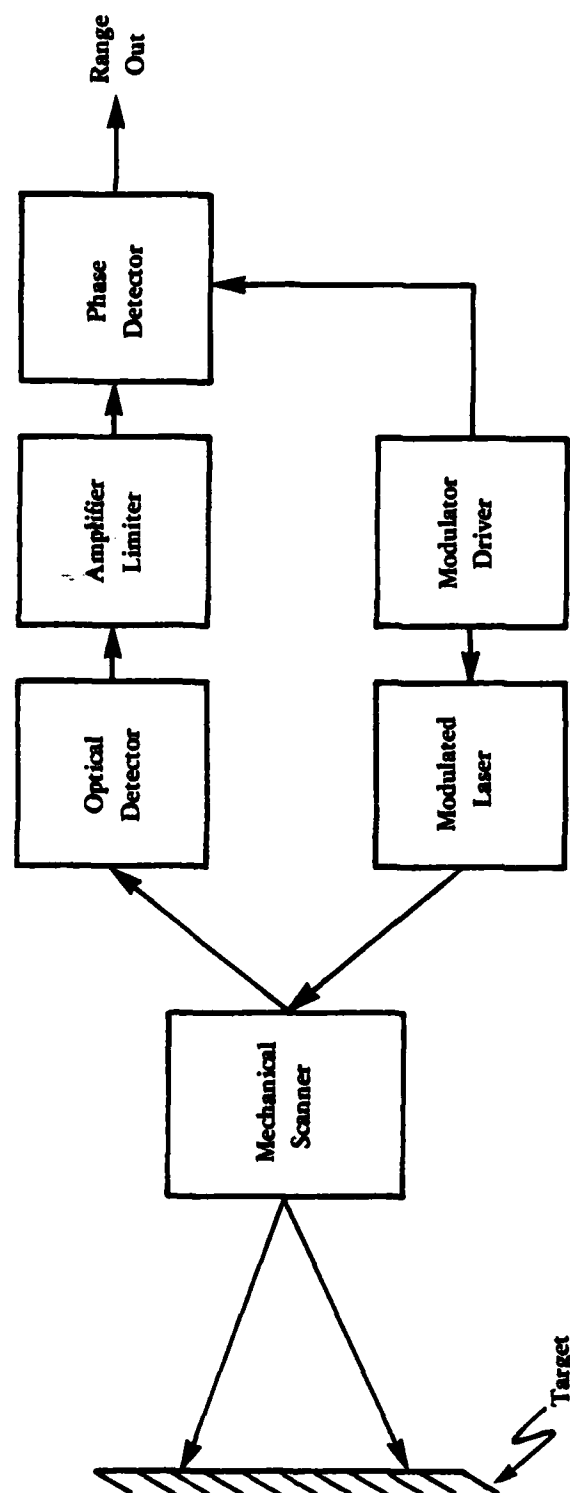


FIGURE 2. BLOCK DIAGRAM OF 3D SENSOR

which is amplified and limited to remove amplitude information inserted by the varying reflectance of the scene. The limited signal contains phase but no amplitude information and is the other input to the phase detector. The output of the phase detector is the phase difference between the reference and reflected signals and corresponds to the range from the sensor to the target.

## 1.2 DATA COLLECTION

One of the tasks of the present program was to collect 3D terrain data similar to that expected from an ASV 3D terrain sensor. While data collection was the main objective of Task I, it was necessary to conduct portions of Task II (defining a sensor) before data could be collected that simulated the real data base. Once a general sensor was defined, the existing tabletop 3D scanner at ERIM was modified to approximate the sensor performed (after scaling) defined under Task II.

The modified, ERIM tabletop 3D sensor was capable of approximating the ASV terrain sensor provided the terrain features were scaled down by a factor of 6. The scaling was necessitated by the modulation frequency of the tabletop source (a mode-locked HeNe laser). The one-sixth scale modelling meant that a terrain model of 24 ft square (7.31 m) fit onto a 4 ft (1.22 m) square board. Thus the terrain could be moved and handled. The features to be modeled were decided during discussions between DARPA, OSU, Battelle and ERIM personnel. It was finally concluded that 4 terrain features were of primary interest: a trail, a steep slope, a ditch, and a cliff. Additional features included a fence, logs, and both large and small rocks.

Four terrain boards were used in pairs to create 10 different scenes. In order to collect 10 scenes using four terrain boards, many of the boards were used more than once. The orientation of terrain

boards next to each other was used to create a different scene. For example, rotating one board 90° provides a different aspect and hence a different scene. Data were collected on each of the 10 scenes. On each scene a number of frames of data was collected (the ASV sensor is a framing sensor). For each frame, the ASV was assumed to be in a level attitude and the sensor was between 4 (1.22) and 8 ft (2.44 m) above the terrain (the height limits of the ASV). Each frame is the same as if the ASV took a step, stopped, and then took another look.

A detailed description of the terrain boards, the scenes made from those boards, and a discussion of the tabletop sensor modifications are presented in Section 2.

### 1.3 SYSTEM STUDY

The goal of Task II was a conceptual design of a terrain sensor tailored to the requirements of the ASV. At the start of the program, the only system constraint was that the terrain sensor must provide a 3D picture of the terrain sensed. The first item under the conceptual design task was the establishment of a set of parameters to act as a design goal for the conceptual design. The setting of parameters occurred during discussions between OSU, Battelle, DARPA, and ERIM personnel. These discussions consisted of an exchange of engineering information on the various aspects of the entire system. The exchange of information resulted in specifications that were realizable and tailored to the unique requirements of the ASV.

Many of the parameters for the terrain sensor were derived from parameters of the ASV. For example, the spatial resolution of the sensor is approximately the size of the ASV's foot. The frame rate (2 frames/sec) came from the maximum anticipated speed of 10 ft/sec (4.87 m/sec) and a desire to take a frame for each step (5 ft) (1.52 m). The volume, weight and power requirements came from reasonable estimates of the available space and power on the ASV.



Once an initial set of parameters derived from the ASV were defined, work began on the conceptual design. Attention was paid to specifics such as wavelength selection, scan type, laser safety and signal-to-noise. It was necessary to balance all of the various goals and specifications against each other to arrive at a final design. A detailed discussion of the design trade-offs is presented in Section 2.

## SECTION 2

### TECHNICAL DISCUSSION

This discussion details the technical work performed under Tasks I and II of the ASV program. The Task I data collection is discussed in two parts: Tabletop Three-Dimensional Sensor (T3DS) sensor improvements, and data collection parameters. The ASV sensor conceptual design, Task II, is discussed next. A summary of the sensor parameters is given in Section 2.2.6.

#### 2.1 TASK I: DATA COLLECTION

Under Task I, simulated ASV terrain sensor data were collected. To collect the data, it was necessary to first modify ERIM's 3D tabletop sensor so that the data from the tabletop sensor would simulate the data from the proposed ASV terrain sensor. Early in the program it was decided that the 3D tabletop sensor could not generate simulated ASV sensor data unless a scale factor of 6 was introduced in the physical size of objects. It was decided to use 1/6 scale models of terrain to collect simulated ASV terrain data.

The tabletop sensor was modified, terrain models built, and data collected. Each of these are discussed in the following text. When dimensions are given, they are the scaled-up or ASV size dimensions. For example, the 4 ft [1.22 m] square terrain modules are referred to as being 24 ft [7.31 m] square.

##### 2.1.1 Sensor Improvements

ERIM's experience with the T3DS indicated that the performance of the sensor could be improved through modifications to the various components.

The phase detector was modified to operate properly across an ambiguity interval and improve its noise characteristics when compared to the existing phase detector. An improved limiting amplifier and a narrowband surface acoustic wave (SAW) bandpass filter were installed to improve the noise performance of the T3DS.

To obtain a noise limit comparable to the proposed ASV sensor, sources of noise in the T3DS system had to be identified and corrected. Three sources of phase noise were identified: the frequency shift local oscillator, the mode-locker oscillator, and the laser itself. To reduce the phase noise from the oscillators, the units were replaced with digital frequency synthesizers. The laser phase noise was generated by two internal mechanisms: low frequency pulsations and self mode-locking at a frequency 80 kHz higher than the natural oscillation frequency of the mode locker block. The low frequency pulsations were reduced by applying r-f modulation to disrupt the pattern. The self mode-locking frequency was adjusted to the block frequency by meticulously shortening the length of the laser cavity. The laser pulse output after this adjustment exhibited a greatly reduced noise component.

Optical and mechanical modifications to the galvanometer scanner were necessitated by the large TFOV (40 x 60 deg) (it was impossible to scan 60 x 60 deg with the present system) and spot size requirements (6 in. [15.2 cm] diameter). The frame holding the galvos was cut down to increase the total field of view and the galvos themselves were enclosed in boxes and their input leads filtered to reduce Radio Frequency Interference (RFI) which was causing erratic motion of the scan mirrors.

A Galilean expansion telescope was designed for the laser output beam. The beam size was 6 in. [15.2 cm] in diameter at 29 ft, [8.84 m]

and 1.5 in. [3.8 cm] in diameter at 8 ft [2.4 m]. The receiver optics were designed to have an FOV several times larger (30 in. [76 cm] diameter) than the spot size. This requirement was necessary since the transmit and receive paths are non-collinear and therefore suffer from variable parallax across the TFOV. The parameters and performance of the modified sensor are presented in Table 1 and agree fairly well with the ASV sensor parameters with the exception of the horizontal FOV.

TABLE 1. TABLE TOP SCANNER PARAMETERS

	<u>3D Table Top</u>	<u>Conceptual Design</u>
Vertical FOV (deg)	60	60
Horizontal FOV (deg)	40	60
Laser Spot Size at 29 ft (8.8 m)	6 in. [15.2 cm]	6 in. [15.2 cm]
Ambiguity Interval (ft)	37.3 [11.38 m]	32 [9.75 m]
Range Resolution (in.)	1.7 [4.32 cm]	2 [5.08 cm]

#### 2.1.2. Scene Modelling and Data Collection

A major portion of Task I was to collect image data of terrain suitable for foot placement algorithm development. Instead of going outside for full scale measurements, it was decided to use 1/6 scale model terrain scenes to collect terrain data.

The spot size varies between 6 in. [15.2 cm] at 30 ft [9.14 m], and 1.5 in. [3.8 cm] at 8 ft [2.44 m]. The footprint of the TFOV with dimensions of 11.5 x 27.5 x 22.5 ft [3.51 x 8.38 x 6.86 m] (W x L x W) on level ground is a trapezoid with the narrow part of the trapezoid closest to the sensor. Figure 3 illustrates the footprint size of the TFOV on a typical scene.

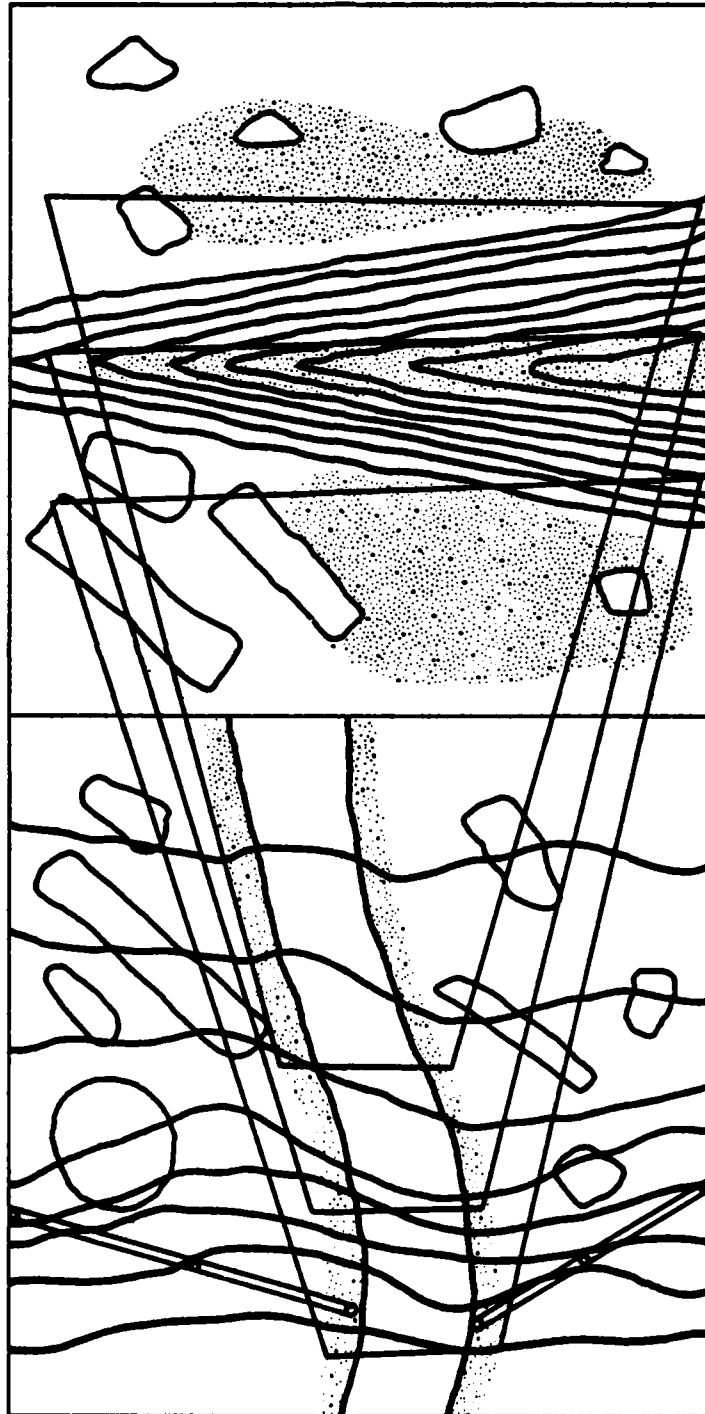


FIGURE 3. TFOV FOOTPRINT SIZE ON TYPICAL SCENE

Based on discussions with DARPA, OSU, and Battelle, requirements were placed on the types of terrain features that should be modeled. The models represented typical topological and surface features found in forest and steep, hilly terrain. The four features selected were: a slope, a trail, a cliff, and a ditch. Surface materials specified were rocks, logs, trees, fence, etc. Within the means available, these materials were placed in reasonable positions and quantities upon the scene models. The basic surface of each module was a mixture of sand and small gravel. Photographs of the modules are shown in Figures 4 to 7.

The size of the scene models was determined by scale and feature requirements. Based on the maximum width of the footprint, 22.5 ft [6.8 m], and the number of features, 4, it was decided to build each feature into an independent 24 ft [7.31 m] square module. Drawings of the four modules are shown in Figures 8 to 11. Table 2 lists the measurements of the permanent surface features.

The slope module (Figure 8) was designed to incorporate grades approaching the ASV maximum design capabilities. Across the module, the slope varies from 36 to 58%; the maximum height is 9 ft (108 inches) [2.74 m]. In nature, few objects would remain on such a slope and for this reason only a few large rocks and logs were used as surface features in this module.

The trail and cliff modules (Figures 9 and 10) incorporate obstacles that the ASV must climb over or onto. In the trail module the fence was built to a height of 3 ft [0.91 m]. This height was a compromise between the 4 ft [1.22 m] maximum climbing height of the ASV and the difficulty involved in modeling a 6 to 8 ft [1.83 to 2.44 m] fence. The 4 ft [1.22 m] step height of the ASV was modeled by the 4 ft [1.22 m] high cliff module. Surface features for these modules included logs, large rocks, small rocks, and a large tree (trunk only) on the trail module.



FIGURE 4. SEMI-OVERHEAD PHOTO — SLOPE MODULE

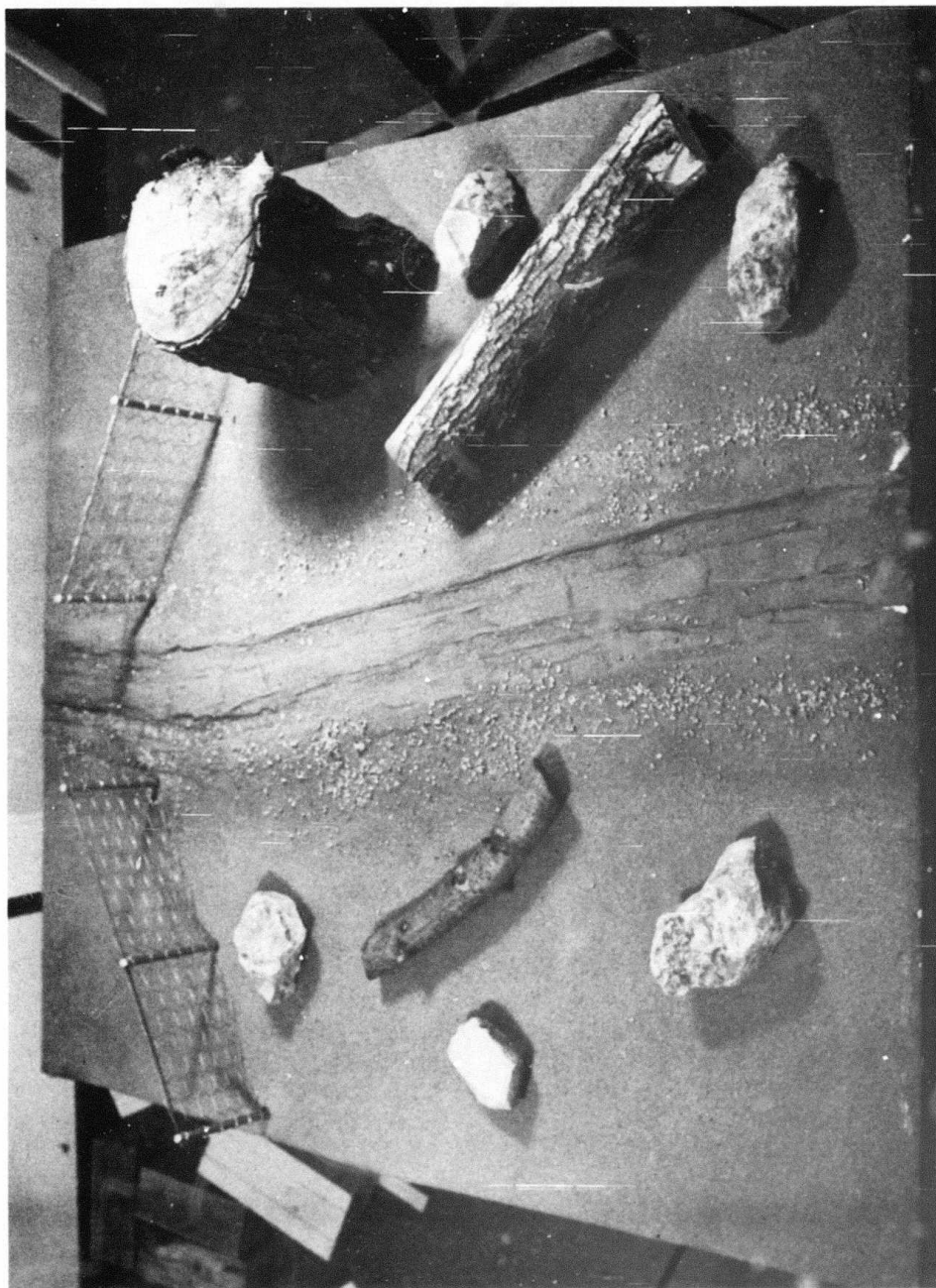


FIGURE 5. SEMI-OVERHEAD PHOTO — TRAIL MODULE





FIGURE 6. SEMI-OVERHEAD PHOTO — CLIFF MODULE

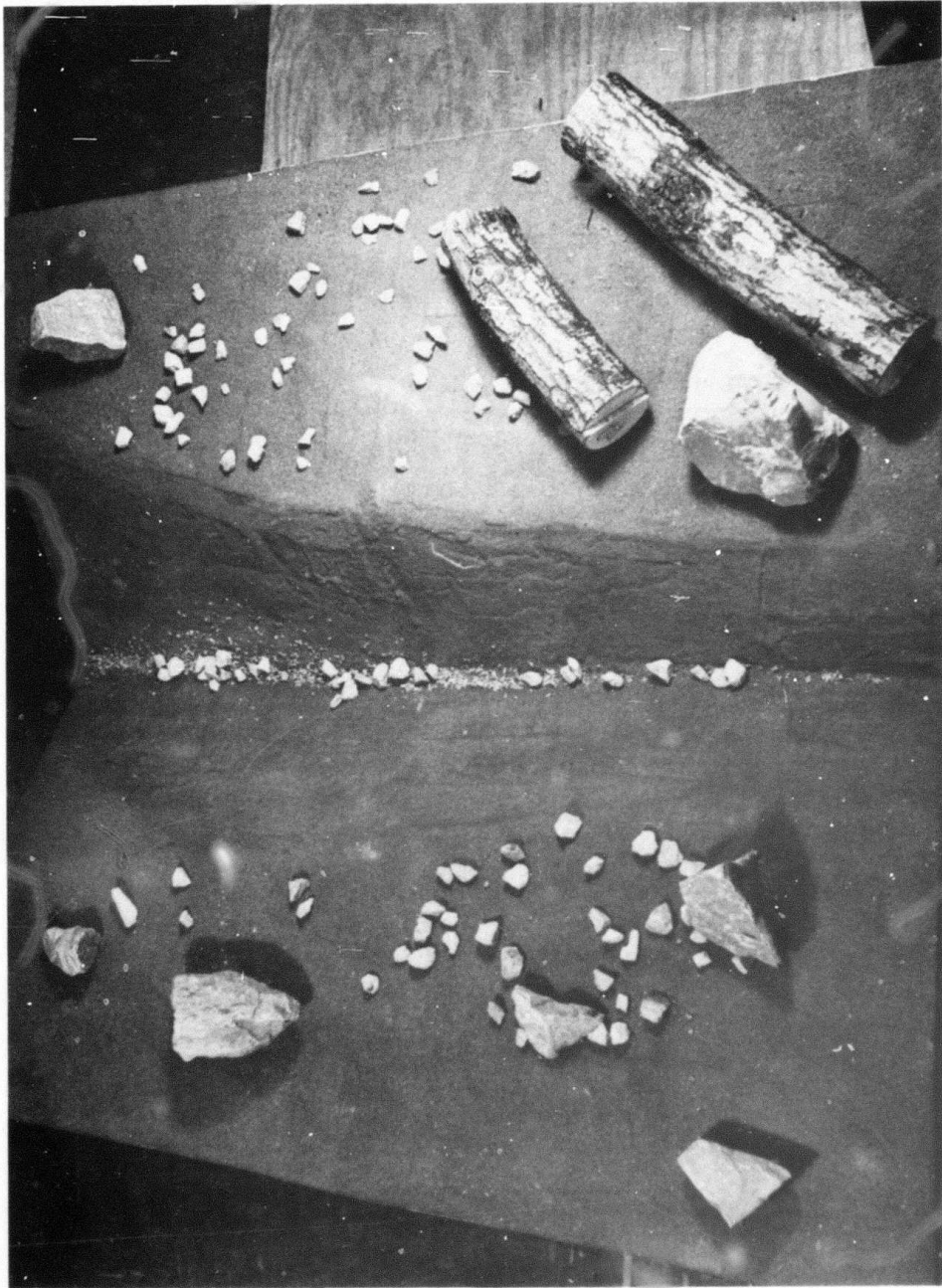
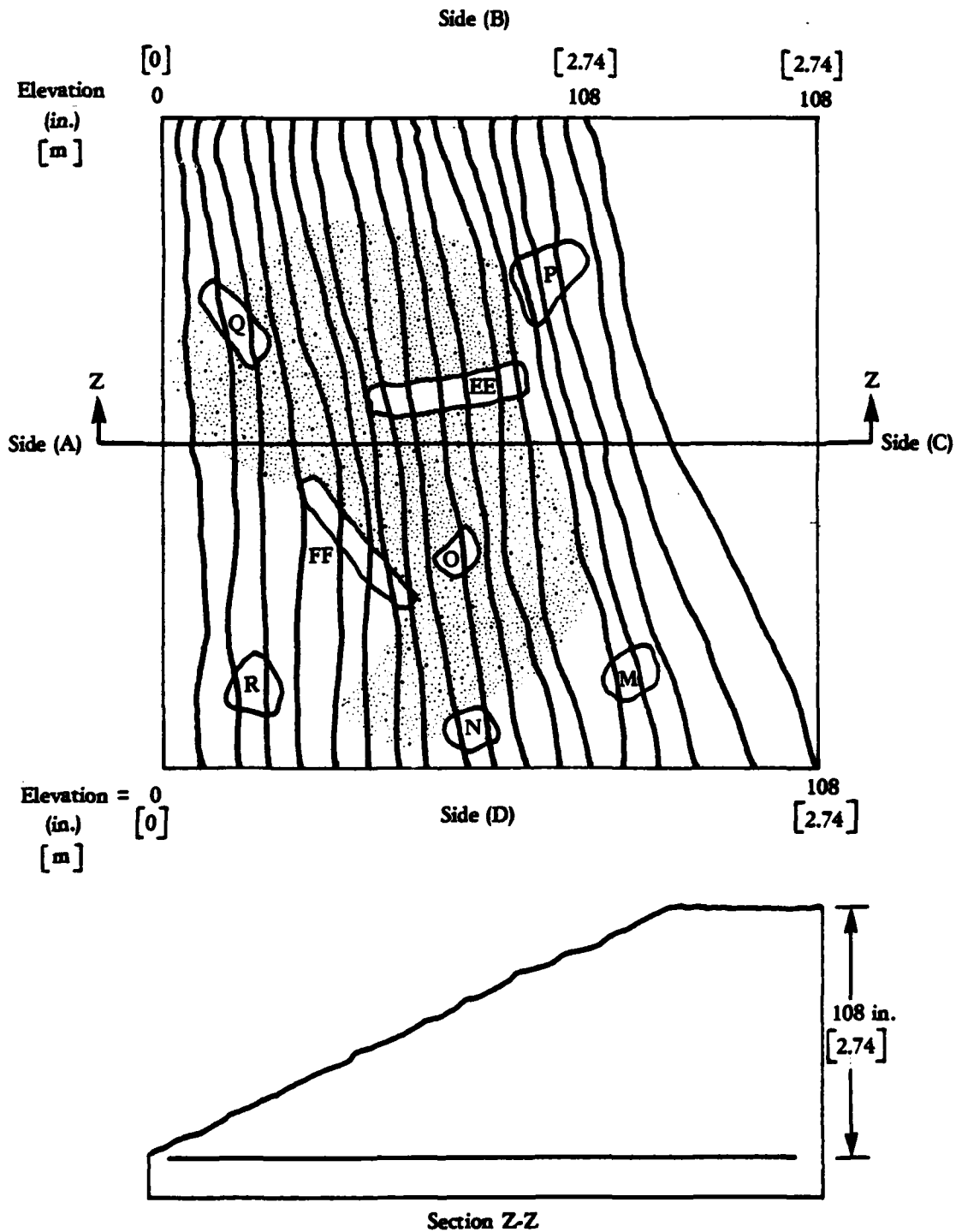
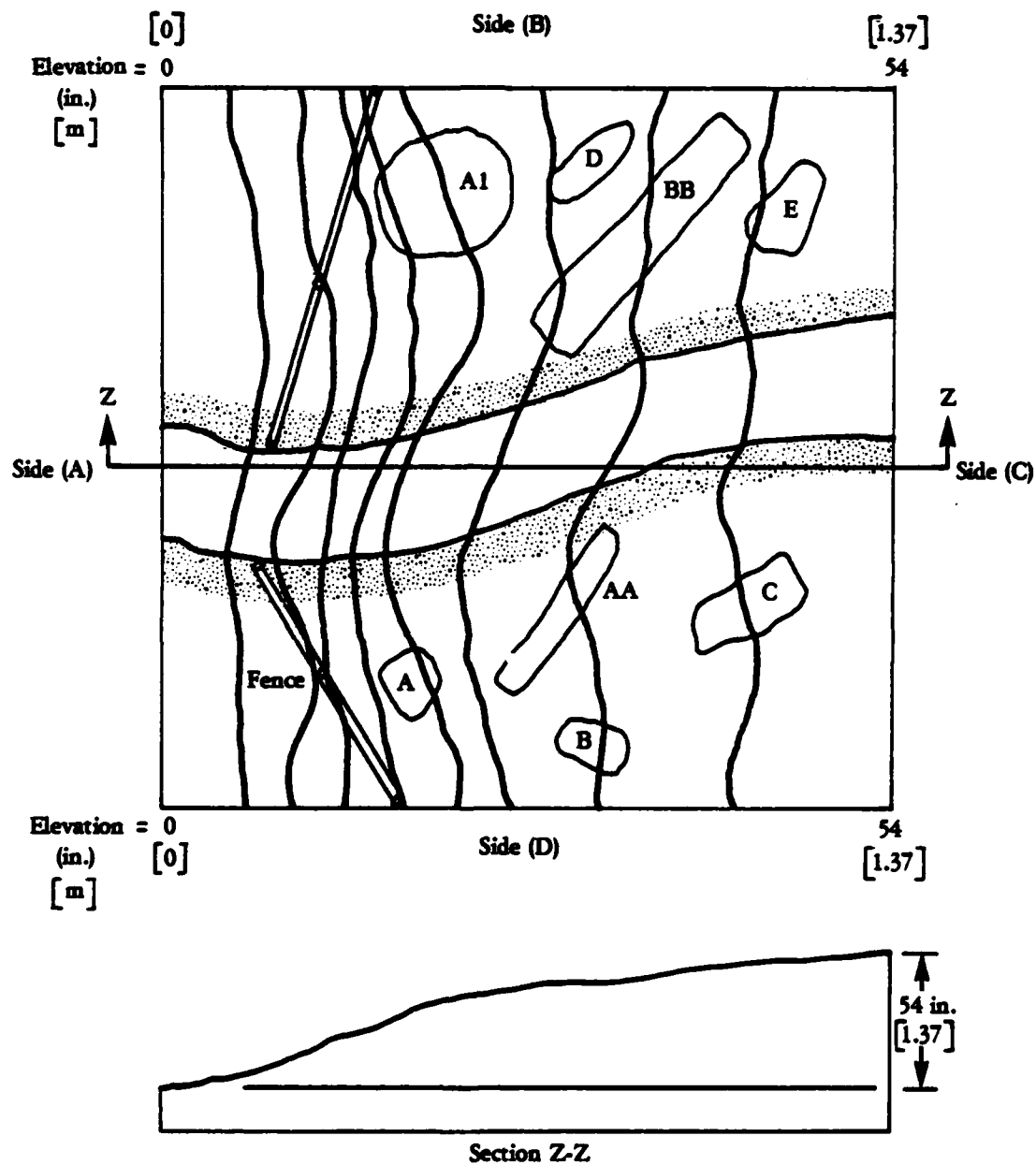


FIGURE 7. SEMI-OVERHEAD PHOTO — DITCH MODULE



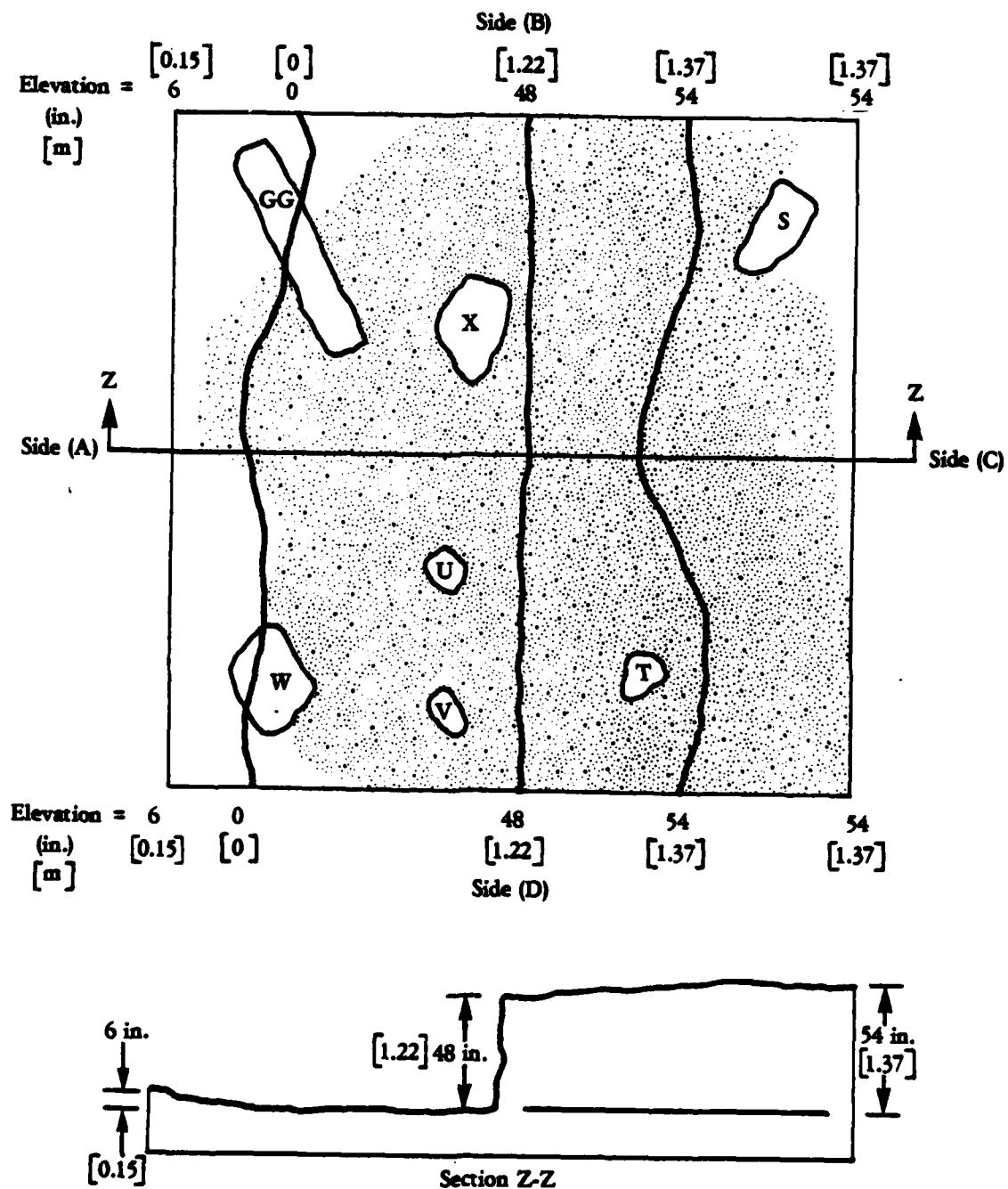
Note: Surface features and positions not to scale.

FIGURE 8. SLOPE MODULE



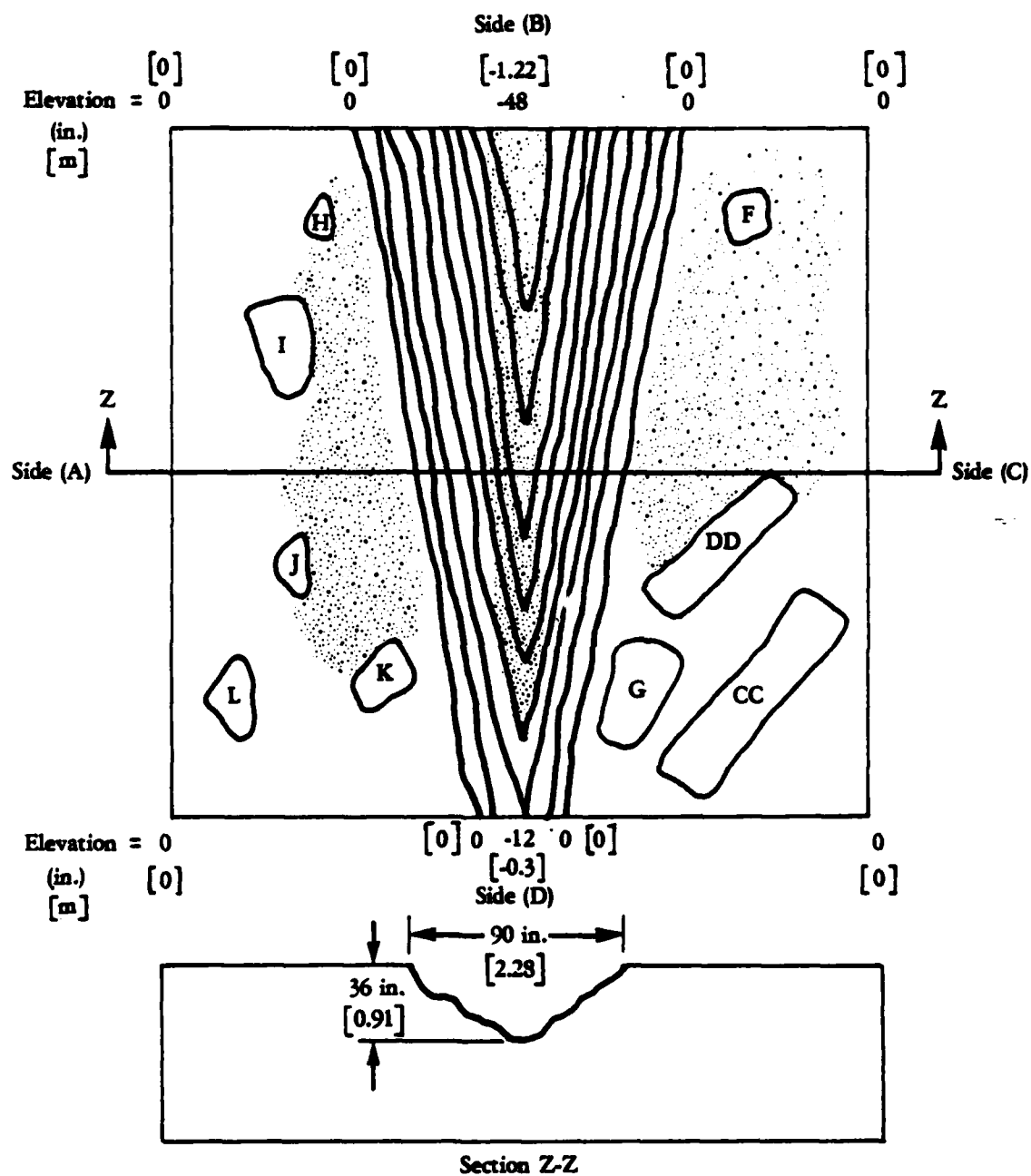
Note: Surface features and positions not to scale.

FIGURE 9. TRAIL MODULE



Note: Surface features and positions not to scale.

FIGURE 10. CLIFF MODULE



Note: Surface features and positions not to scale.

FIGURE 11. DITCH MODULE

TABLE 2. APPROXIMATE SIZES OF SCENE SURFACE MATERIALS  
(Dimensions are Actual Equivalent Sizes)

ROCKS

	<u>Height</u> (in)[cm]	<u>Width</u> (in)[cm]	<u>Length</u> (in)[cm]
A	18 [45.7]	19.5 [49.5]	30 [76.2]
B	6 [15.2]	18 [45.7]	24 [61.0]
C	13.5 [34.3]	24 [61.0]	42 [106.7]
D	21 [53.3]	21 [53.3]	30 [76.2]
E	16.5 [41.9]	16.5 [41.9]	37.5 [95.3]
F	12 [30.5]	21 [53.3]	21 [53.3]
G	33 [83.8]	30 [76.2]	42 [106.7]
H	15 [38.1]	15 [38.1]	19.5 [49.5]
I	24 [61.0]	27 [68.6]	28 [71.1]
J	10.5 [26.7]	15 [38.1]	19.5 [49.5]
K	19.5 [49.5]	22.5 [57.2]	27 [68.6]
L	13.5 [34.3]	21 [53.3]	19.5 [49.5]
M	16.5 [41.9]	18 [45.7]	24 [61.0]
N	12 [30.5]	19.5 [49.5]	21 [53.3]
O	12 [30.5]	19.5 [49.5]	21 [53.3]
P	24 [61.0]	21 [53.3]	30 [76.2]
Q	16.5 [41.9]	15 [38.1]	33 [83.8]
R	16.5 [41.9]	21 [53.3]	22.5 [57.2]
S	16.5 [41.9]	22.5 [57.2]	36 [91.4]
T	13.5 [34.3]	19.5 [49.5]	24 [61.0]
U	10.5 [26.7]	16.5 [41.5]	22.5 [57.2]
V	15 [38.1]	18 [45.7]	25.5 [57.2]
W	25.5 [64.8]	30 [76.2]	45 [114.3]
X	39 [99.1]	33 [83.8]	39 [99.1]

TABLE 2. APPROXIMATE SIZES OF SCENE SURFACE MATERIALS (Cont)  
(Dimensions are Actual Equivalent Sizes)

LOGS		
	<u>Length</u>	<u>Diameter</u>
AA	75 [190.5]	10.5 [26.7]
BB	103.5 [262.9]	21 [53.3]
CC	96 [243.8]	21 [53.3]
DD	64.5 [163.8]	21 [53.3]
EE	72 [182.9]	12 [30.5]
FF	69 [175.3]	9 [22.9]
GG	93 [236.2]	21 [53.3]

TREE TRUNK		
	<u>Length</u>	<u>Diameter</u>
A1	60 [152.4]	45 [114.3]

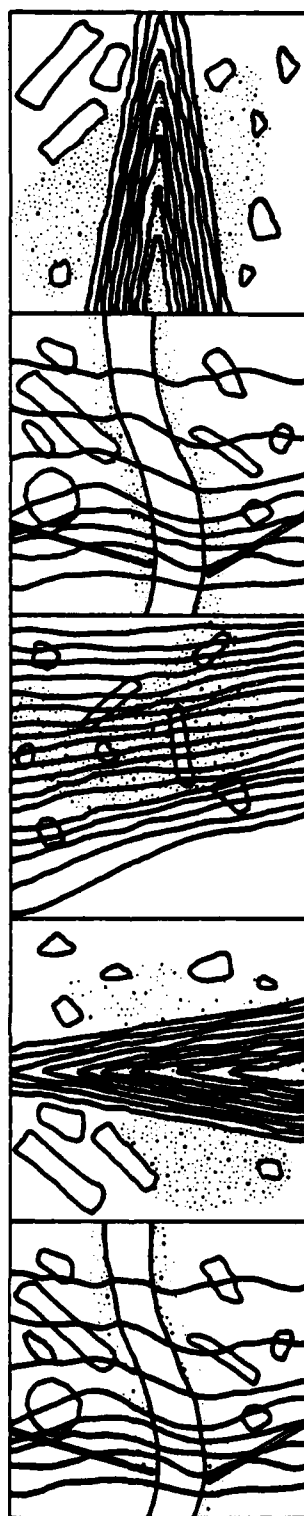


The ASV must also traverse or avoid holes, ravines, and natural or man-made ditches. This type of obstacle was modeled by the ditch module (Figure 11). The V-shaped ditch slopes down and widens across the module providing a variation in depth and width with crossing position. At its narrowest the ditch is approximately 2 ft [0.61 m] wide x 1 ft [0.30 m] deep and expands to 16 ft [4.88 m] wide x 4 ft [1.22 m] deep. Surface features include logs, large rocks, and small rocks.

This modular approach also allowed investigators to put the modules alongside each other to create new scenes. Ten of these unique scenes were constructed. Each scene consisted of 2 modules. At a minimum, 3 frames (assuming an ASV step of 5 ft [1.52 m]) could be recorded on a horizontal two-module scene. Of the 10 scenes constructed, it was decided to provide 8 footprints. In some cases this number could be recorded on two scenes due to the upward slope. If this was not possible, a third module was added. In addition, scene 1 was configured using 5 modules (2 modules used twice) to provide a continuous sequence of 14 frames which included a downhill slope. Sketches of these scenes are shown in Figures 12 to 21. Table 3 is a scene matrix table.

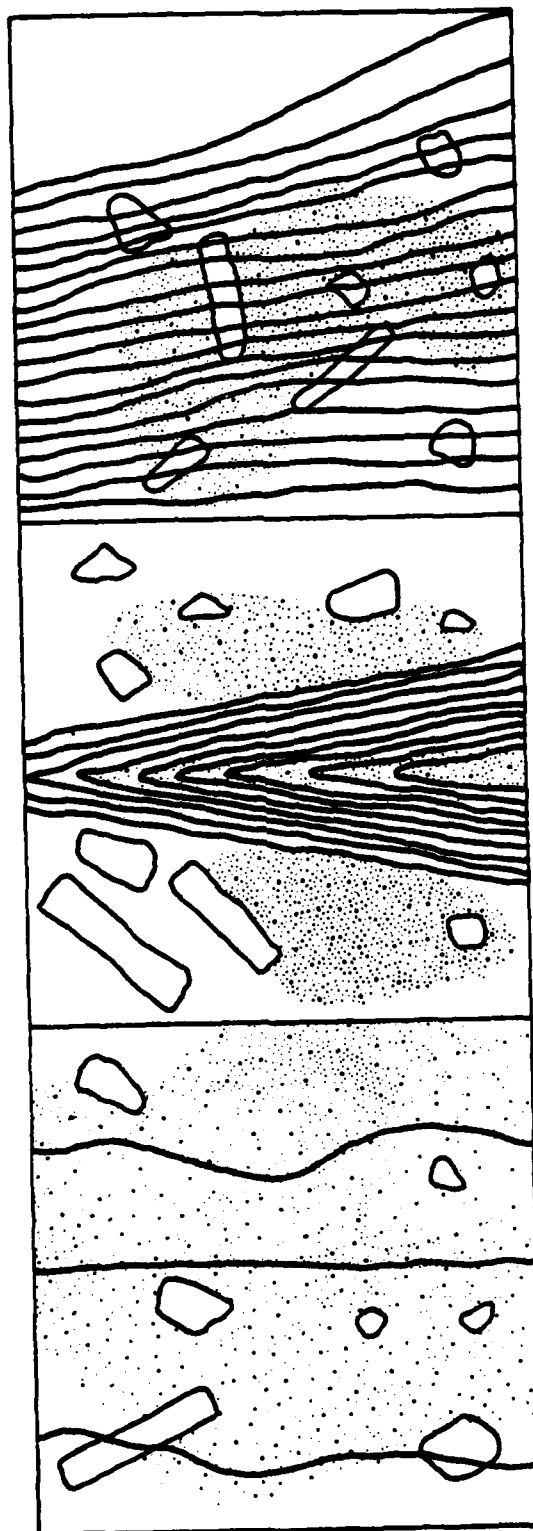
Figure 22 is a photograph of scene 10 and Figure 23 is a collection of 4 frames of data taken on scene 10. The 4 frames are arrayed with the first frame in the upper left, the second in the upper right, the third in the lower left and the fourth in the lower right. In these range images, white is closer to the sensor and dark is further away.

It is impossible to display in this printed reproduction the full dynamic range present in the present data. Despite this limitation, some interesting features can be observed in Figure 23. At the very top of the first frame, one can pick out a log. This log is in the center of the terrain board (Figure 22). The log is also in the



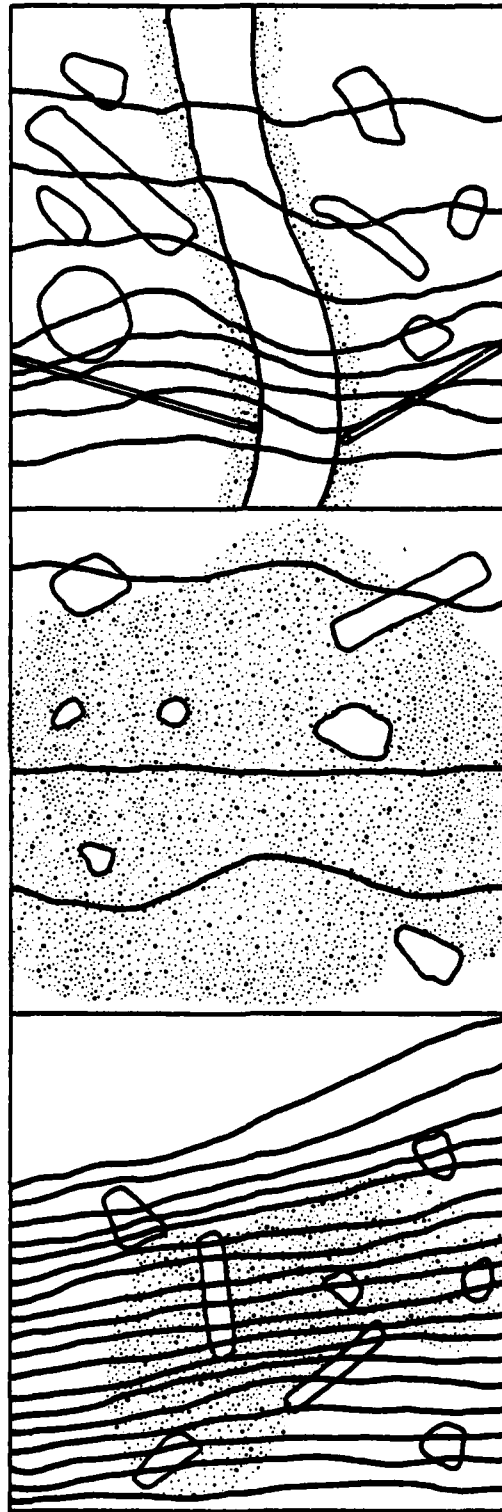
Direction of Scanner Motion →

FIGURE 12. SCENE 1 MODULE CONFIGURATION



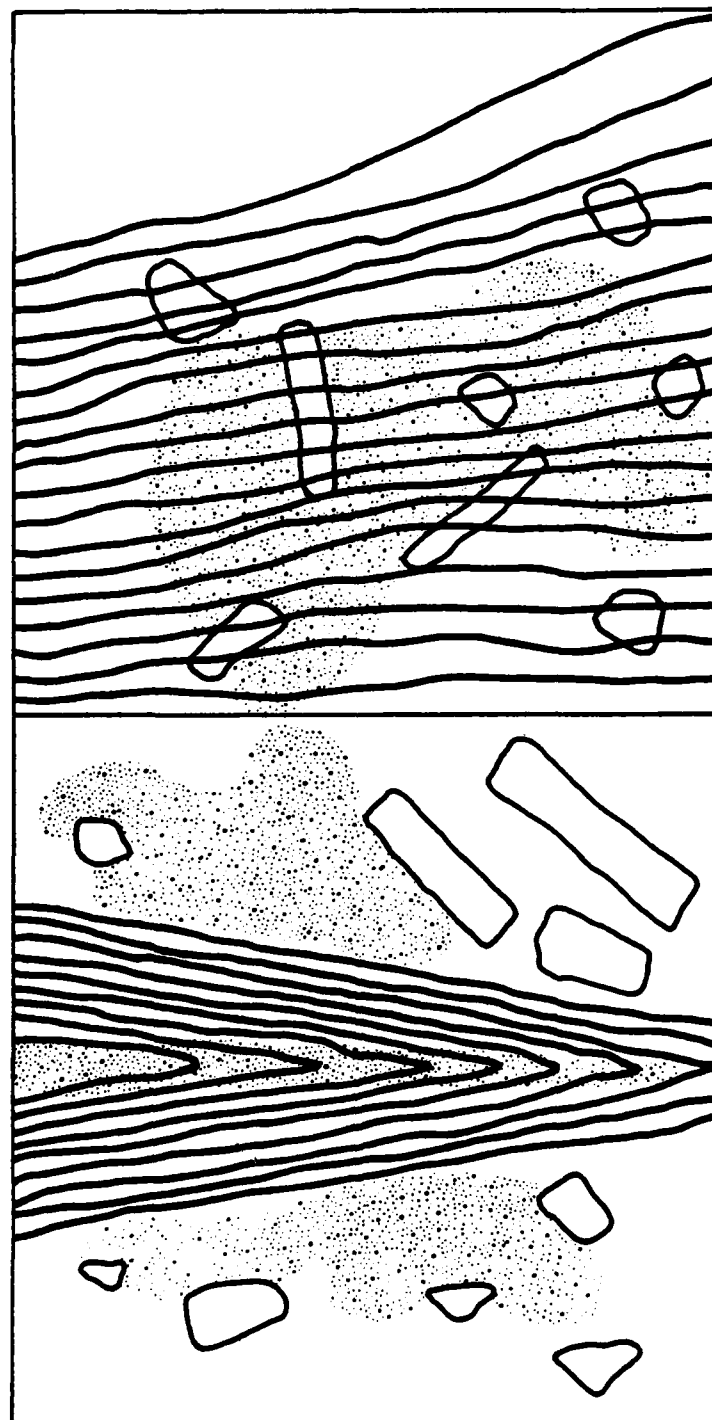
Direction of Scanner Motion →

FIGURE 13. SCENE 2 MODULE CONFIGURATION



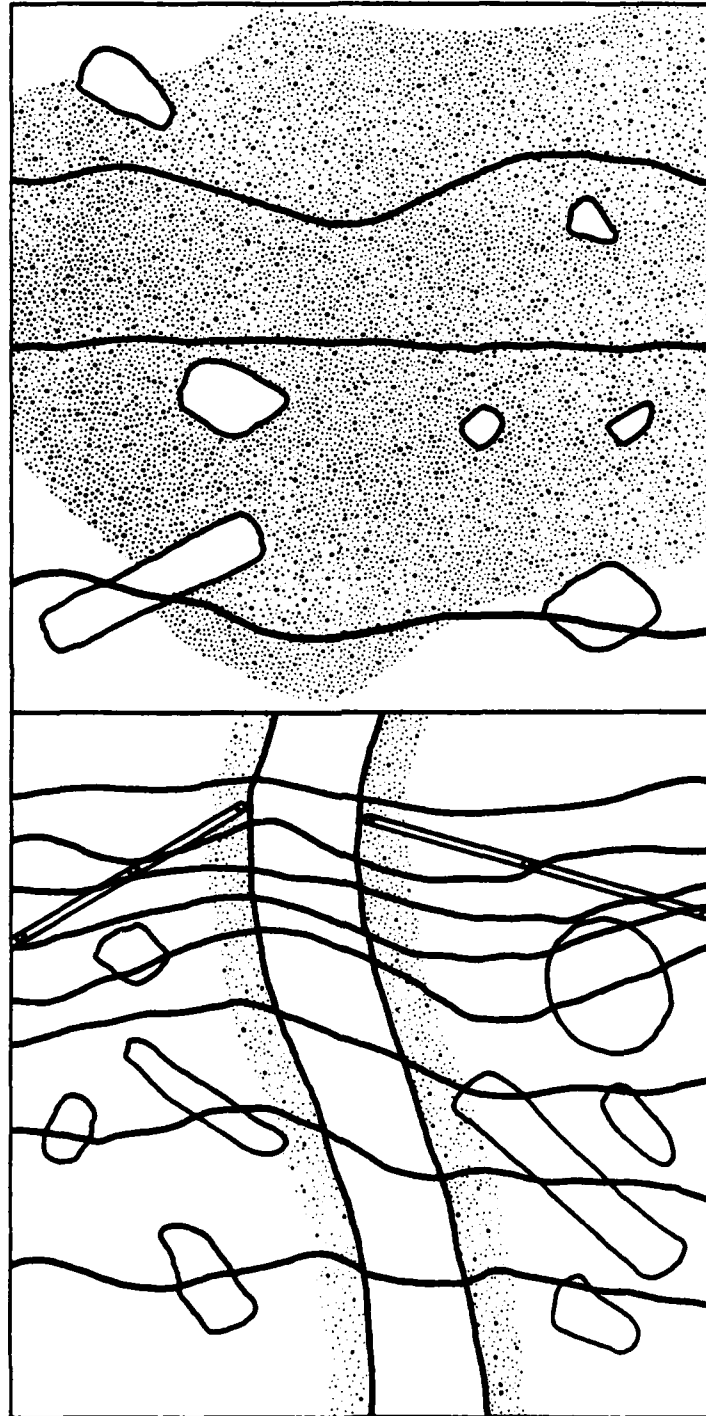
Direction of Scanner Motion →

FIGURE 14. SCENE 3 MODULE CONFIGURATION



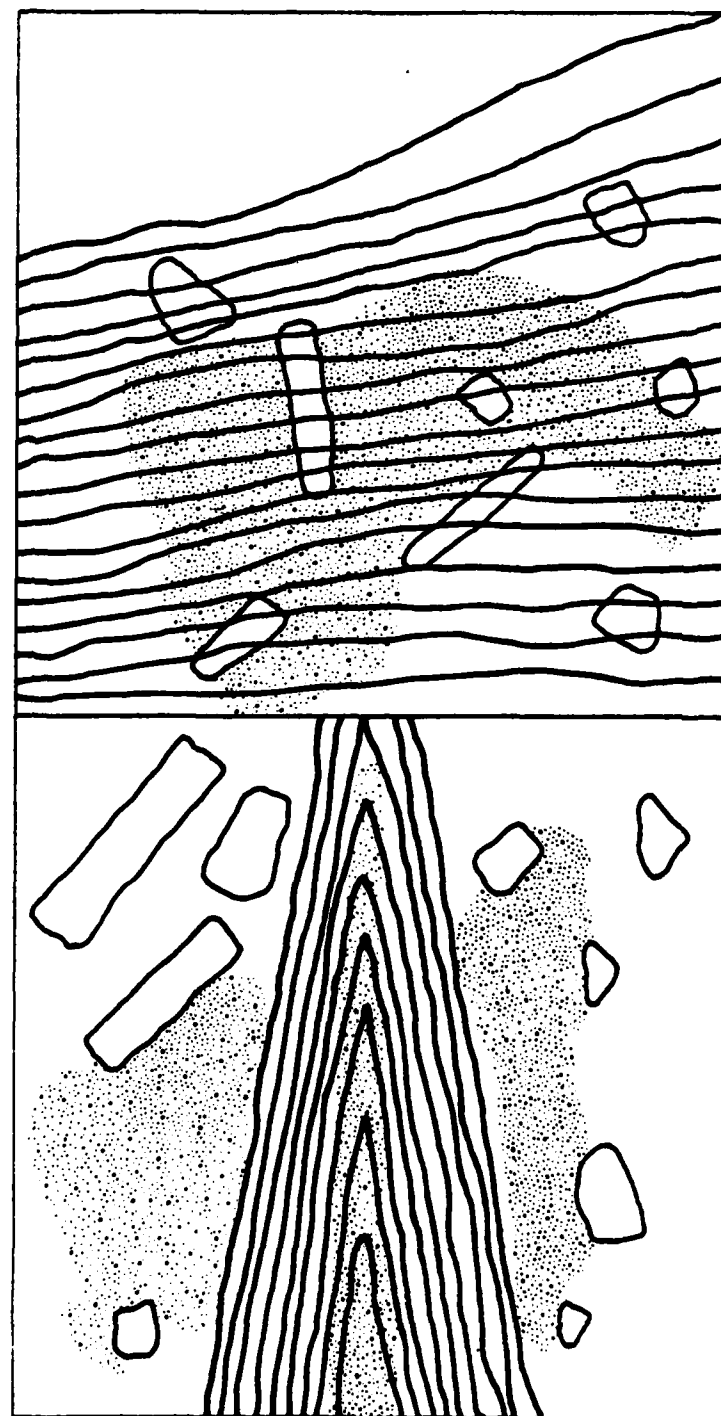
Direction of Scanner Motion →

**FIGURE 15. SCENE 4 MODULE CONFIGURATION**



Direction of Scanner Motion →

FIGURE 16. SCENE 5 MODULE CONFIGURATION



Direction of Scanner Motion →

FIGURE 17. SCENE 6 MODULE CONFIGURATION

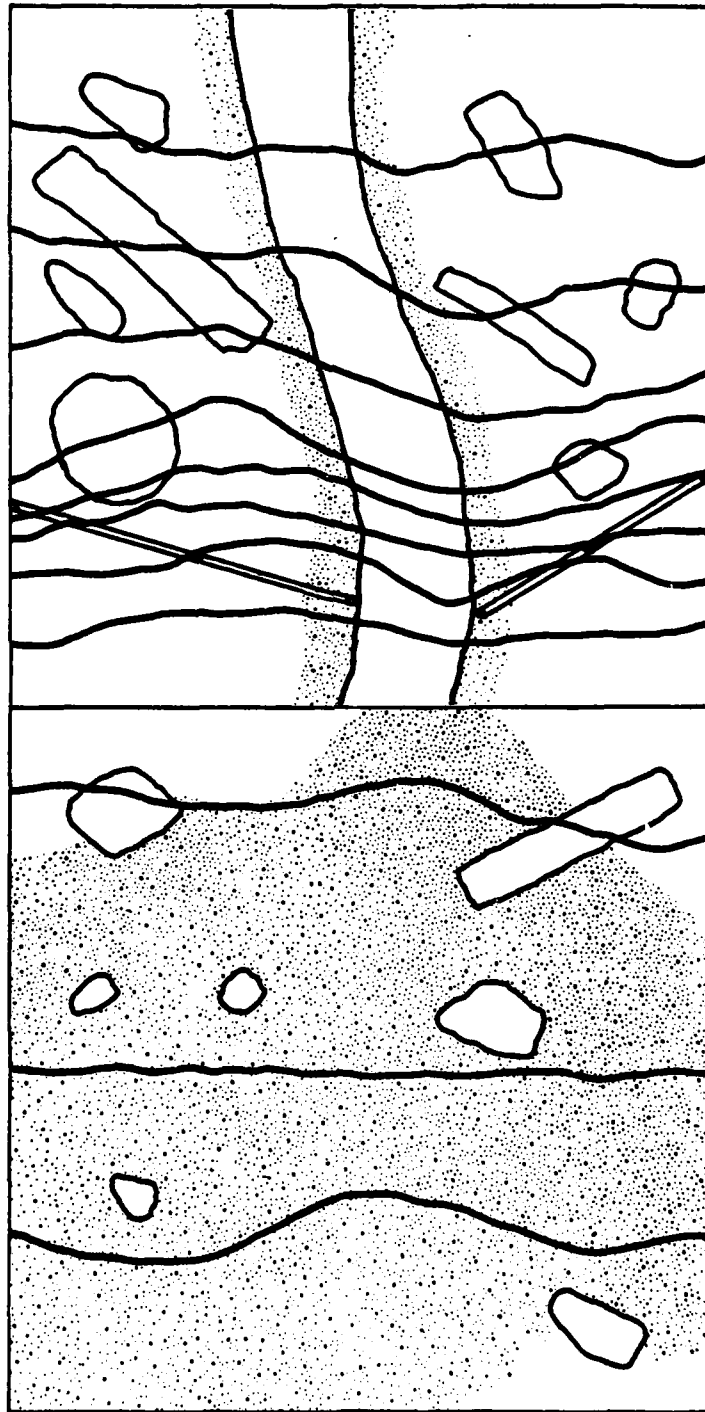


FIGURE 18. SCENE 7 MODULE CONFIGURATION



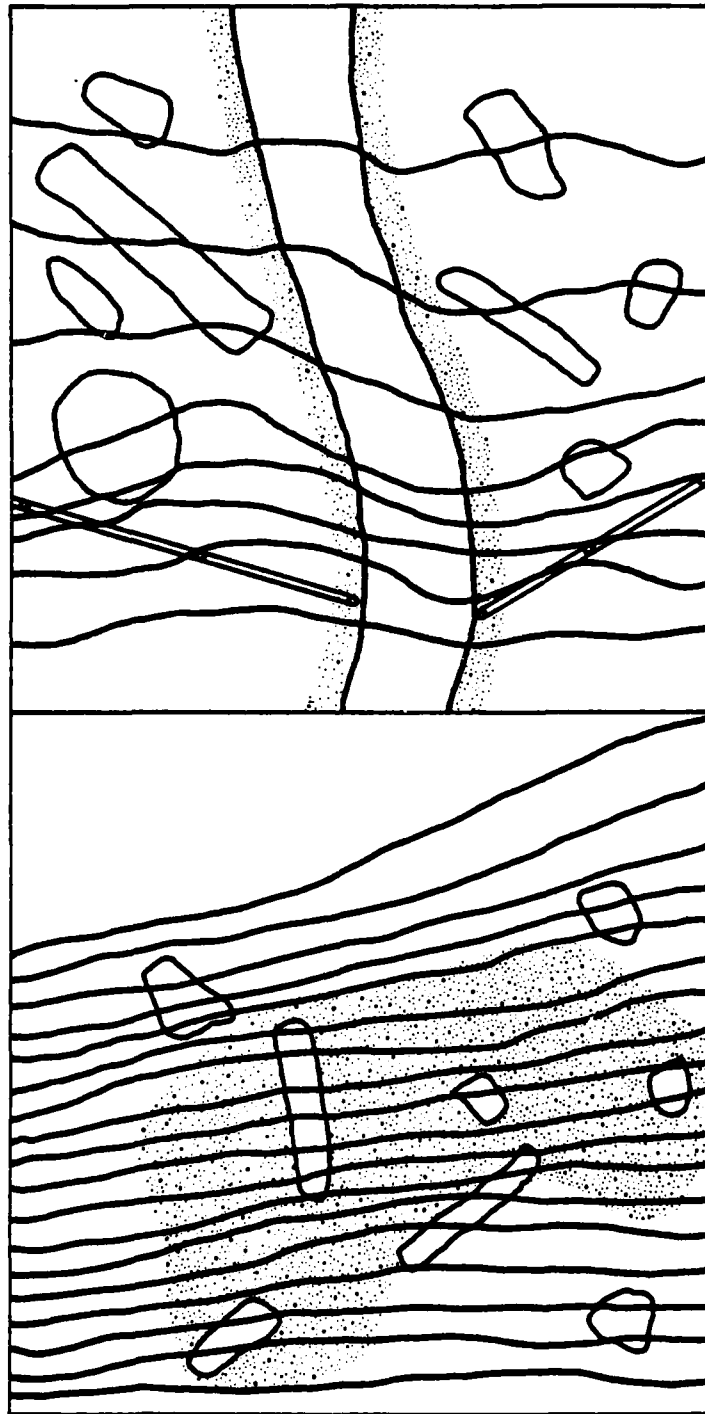
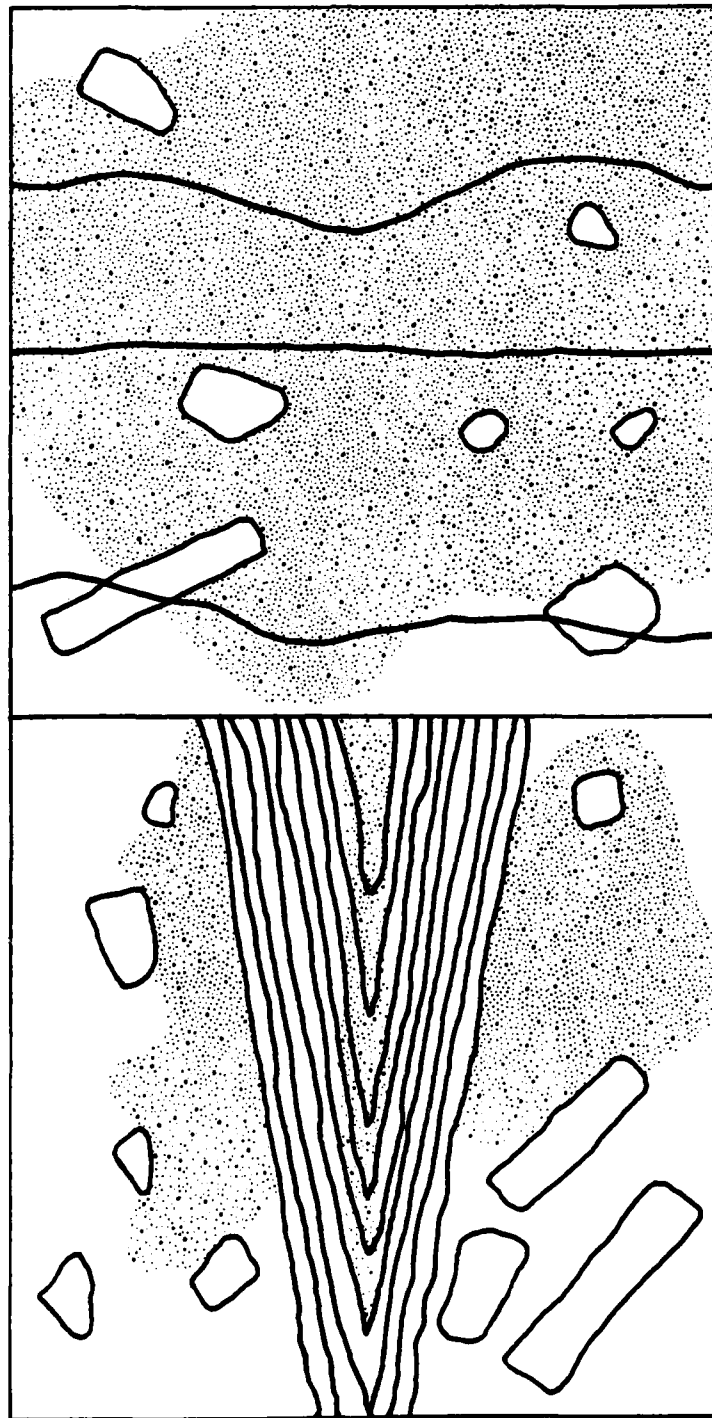
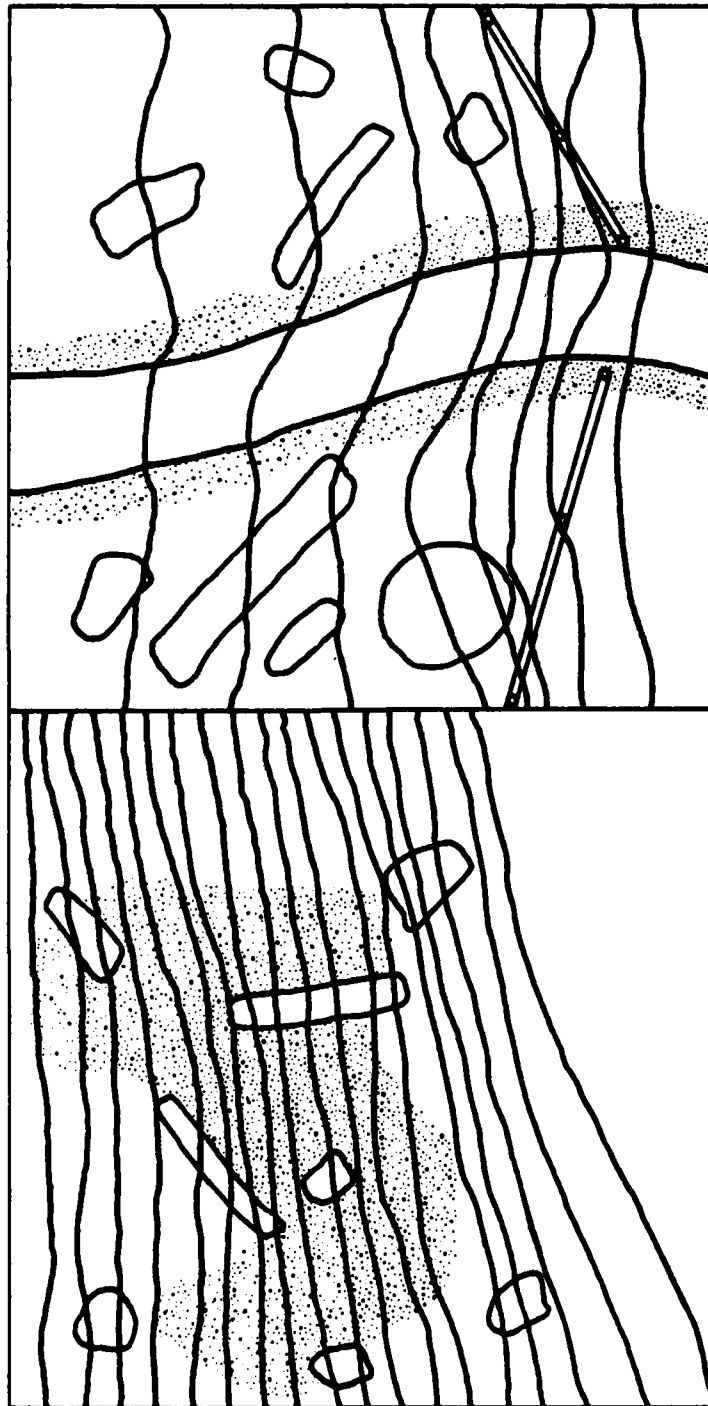


FIGURE 19. SCENE 8 MODULE CONFIGURATION



**FIGURE 20. SCENE 9 MODULE CONFIGURATION**



Direction of Scanner Motion →

FIGURE 21. SCENE 10 MODULE CONFIGURATION

TABLE 3. SCENE MATRIX

<u>Scene Number</u>	<u>Modules</u>	<u>Orientation</u> <u>(Adjoining Sides)*</u>	<u>Figure</u> <u>Number</u>
1	Trail/Ditch/Slope/ Trail/Ditch	(C/C)(A/C)(A/A)(C/B)	12
2	Cliff/Ditch/Slope	(C/C)(A/A)	13
3	Slope/Cliff/Trail	(C/C)(A/A)	14
4	Ditch/Slope	(C/A)	15
5	Trail/Cliff	(A/A)	16
6	Ditch/Slope	(D/A)	17
7	Cliff/Trail	(A/A)	18
8	Slope/Trail	(C/A)	19
9	Ditch/Cliff	(B/A)	20
10	Slope/Trail	(B/B)	21

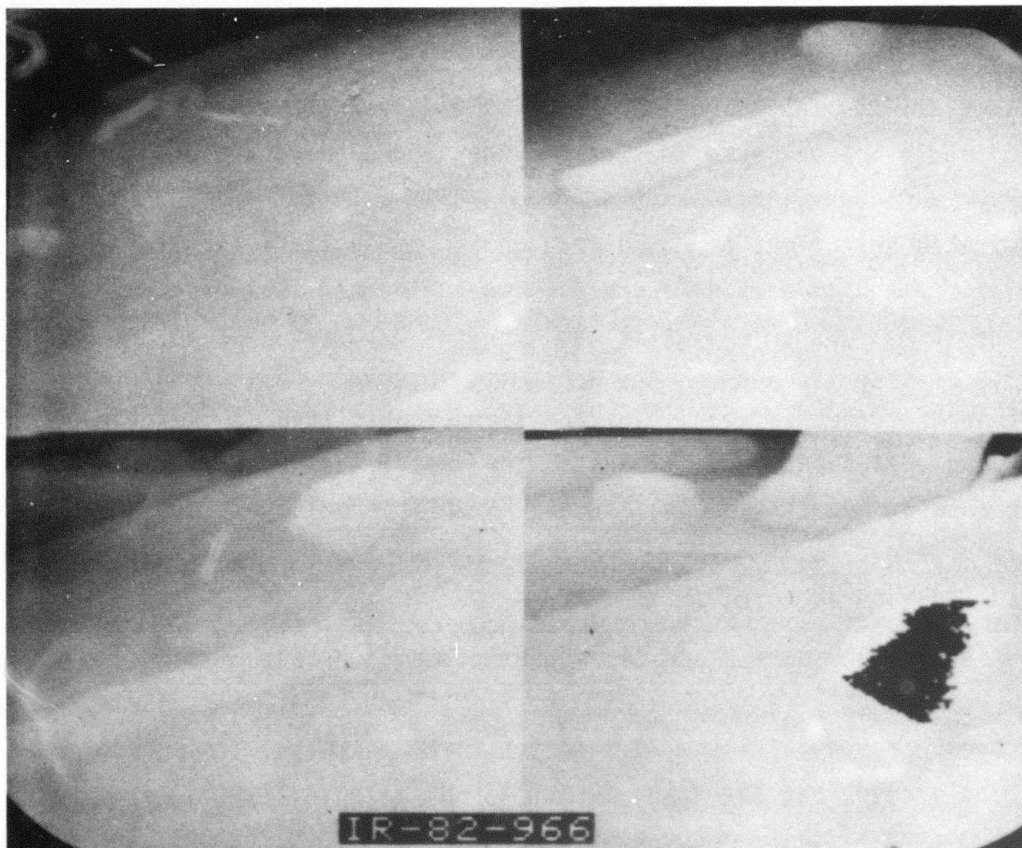
\*See Figures 8-11 for identification of edges.



FIGURE 22. PHOTOGRAPH OF SCENE 10 LOOKING IN DIRECTION OF SCANNER MOTION

Footprint 1

Footprint 2



Footprint 3

Footprint 4

FIGURE 23. RANGE DATA IMAGE OF SCENE 10 FOOTPRINTS 1 THROUGH 4

second frame and the rock above it is also visible. In the second frame, the second terrain board is visible in the upper left hand corner\*. In comparing the photo to the ASV data, one must realize that the ASV data have much coarser resolution and some geometric distortion because the FOV footprint is a trapezoid and the display is rectangular. In the third image the log and rock are again identifiable but now some features in the second board are also observable. Above the rock is a tree trunk. The fourth image illustrates the effect of going through the ambiguity interval. The rock in frame 3 is dark in frame 4 which would seem to indicate that part of it is further away. It isn't. What happened is that the rock got closer than the node in the ambiguity interval and therefore some of it appears further away. The position of this node can be changed by adding a bias to every element in the data if desired. The sudden appearance of something being far away when it should be close could possibly be used as a warning flag telling the operator that the ASV is too close to an object.

A second photograph and accompanying set of data are shown in Figures 24 and 25. In Figure 25, the frames represent walking down the terrain shown in Figure 24. In the first frame the fence posts are barely discernable and the fence is basically invisible. The fence becomes visible in the second image. In the third image the fence is closer and objects beyond it are becoming visible. By the fourth frame the ASV is about to pass through the gate in the fence and other objects which are part of the second terrain board are visible. In all of the images, if the display were to be set up differently, objects in the foreground or background would become visible. The lack of detail in the figures presented is the result of

---

\*Note that the dark background area in the first frame does not appear to have any detail or structure. The detail is there, it just doesn't show in this reproduction.

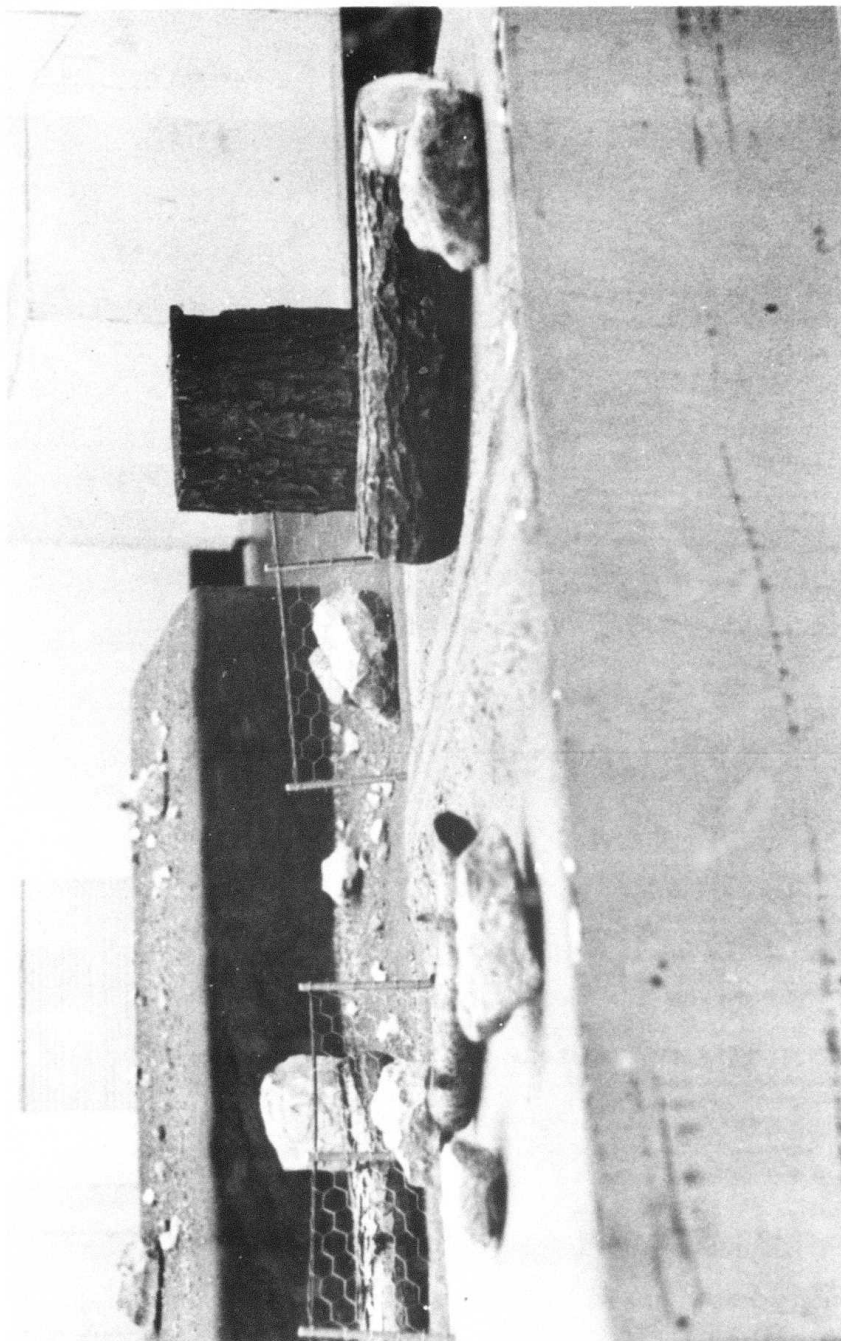
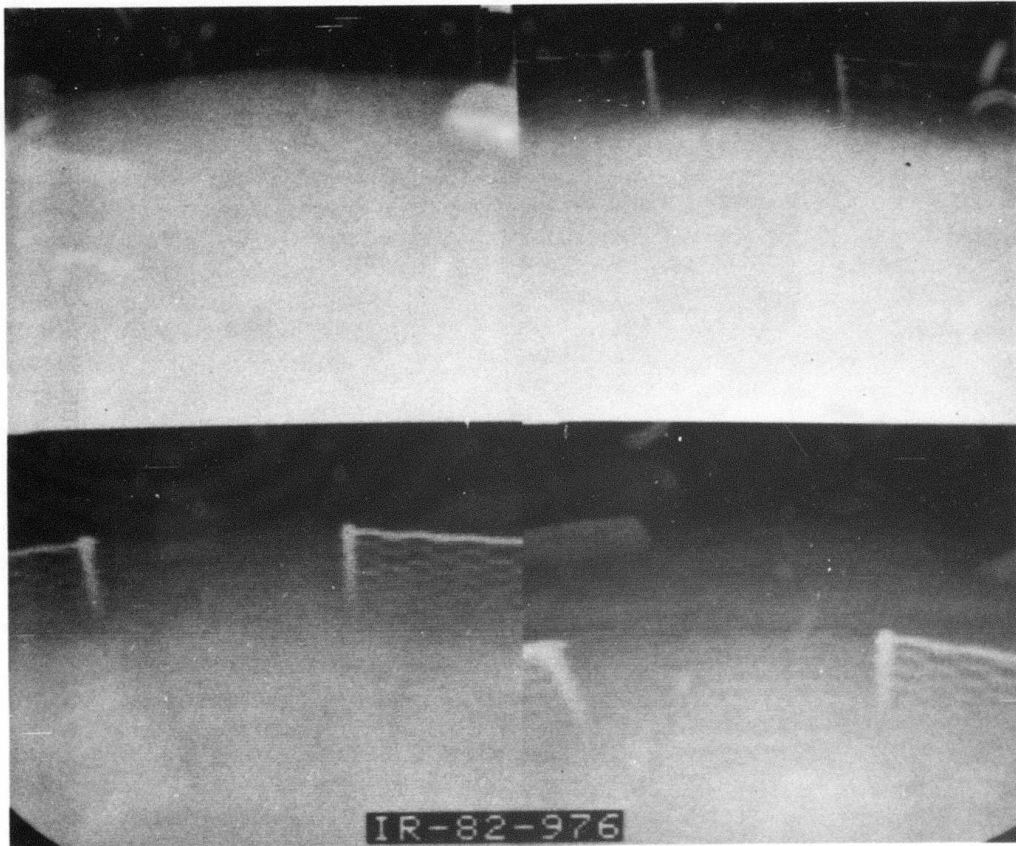


FIGURE 24. PHOTOGRAPH OF SCENE 5 LOOKING IN DIRECTION OF SCANNER MOTION



Footprint 1

Footprint 2



Footprint 3

Footprint 4

FIGURE 25. RANGE DATA IMAGE OF SCENE 5 FOOTPRINTS 1 THROUGH 4

limitations in the printing reproduction process, not limitations in the data.

Data can be presented in other than grey scale images. An alternate representation is presented in Figure 26. In Figure 26 a photo of the scene taken from roughly the same aspect as the image shown below the photo and a plot of a single line of data are all presented in a single figure. The range image and the line plot are on the same horizontal scale and the area from where the line was taken is shown on the image. By comparing the range image and the plot one can see that there is a significant amount of detail that is obscured in the grey scale reproduction process.

As stated in the section on sensor improvements, several optical-mechanical modifications were made to the sensor. Since the ASV sensor operates at a height of 8 ft [2.44 m] it was necessary to elevate the T3DS sensor through the use of a bridge. As shown in Figure 27, the bridge was designed to suspend the sensor above the scenes at a fixed height. Changing the height between the sensor and scenes was performed by changing the scene supporting structures. It should be noted that as slopes were encountered in the scenes the scaled height was allowed to vary from 4 to 8 ft [1.22 - 2.44 m].

The orientation of the sensor with respect to the horizontal remained fixed throughout the data collection (Figure 28). It was possible to alter this orientation (pitch), but without prior knowledge of the vehicle's attitude characteristics while maneuvering, a horizontal position could most likely be assumed. The forward motion of the ASV was simulated by moving the scenes under the sensor in the opposite direction of travel. Based on a forward speed of 10 ft/sec [3.05 m/sec] and a frame rate of 2 per second, a step motion of 5 ft [1.52 m] between scenes was used.

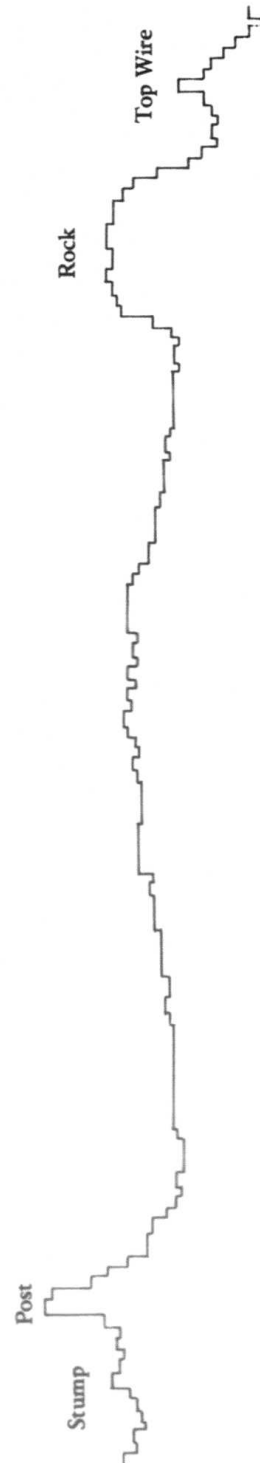
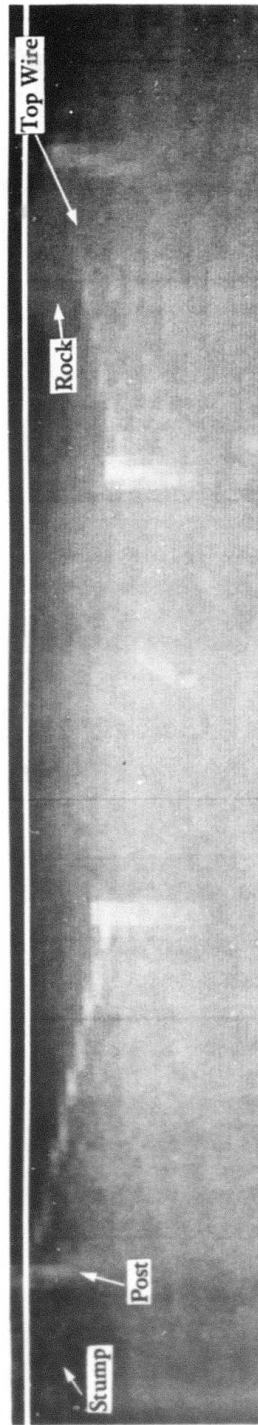


FIGURE 26. PHOTO OF SCENE, A RANGE IMAGE OF THAT SCENE AND A LINE PLOT SHOWING DETAIL IN THE RANGE DATA

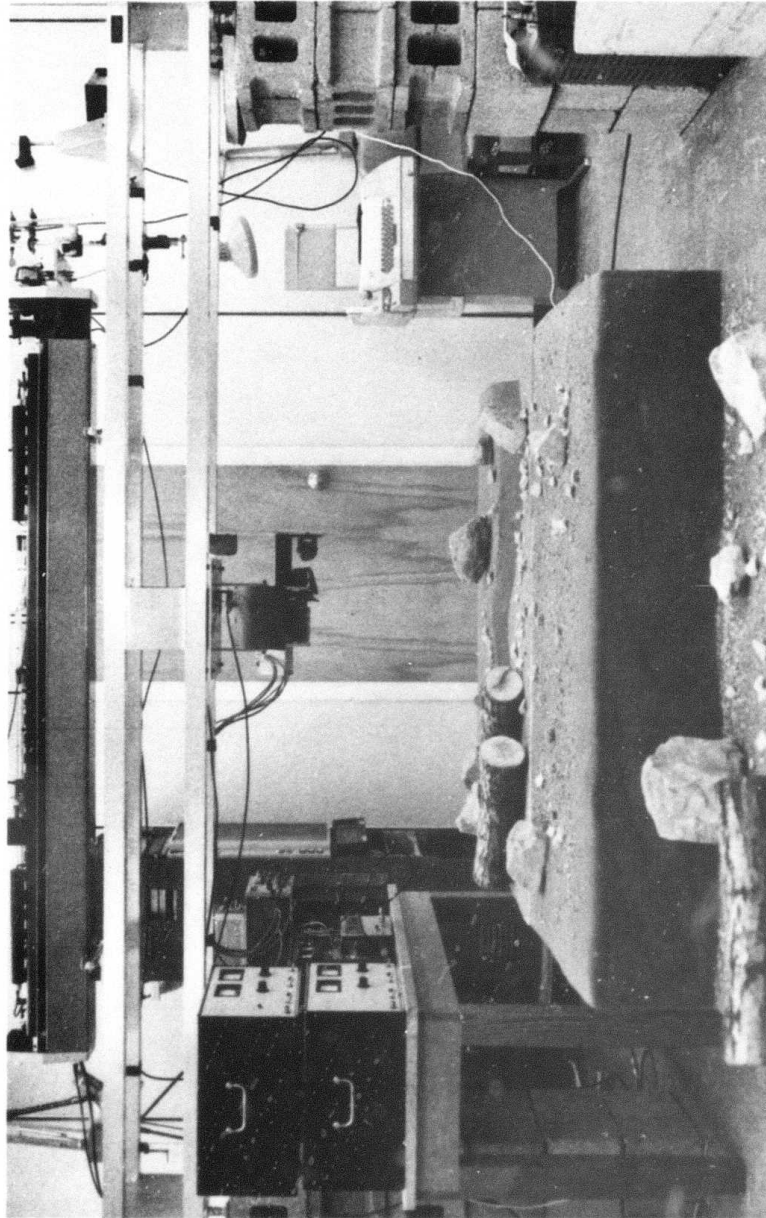


FIGURE 27. SENSOR BRIDGE AND SCANNER ELECTRONICS

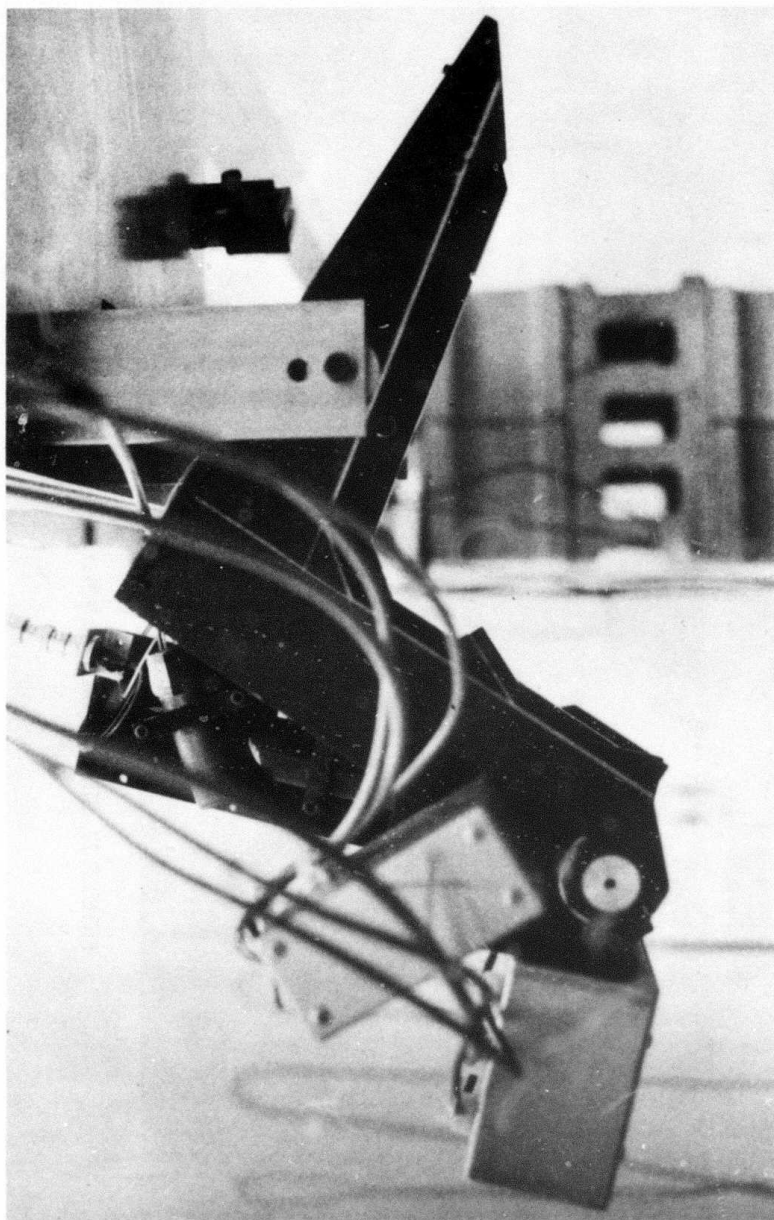


FIGURE 28. SCANNER HORIZONTAL POSITION

The ambiguity interval of the sensor was 37.3 ft [11.37 m]. As shown in Figure 29, the length of this interval was sufficient to ensure that an entire horizontal footprint was within this interval. The leading edge of this interval was manually set 2 ft [0.61 m] from the bottom of the sensor frame, Figure 30. The reference point of the sensor was assumed to be the vertical scan mirror and as can be seen in Figure 30 the leading edge of the ambiguity interval was 3.4 ft [1.04 m] from its surface. In some of the scenes the sensor distance to the surface is reduced below 3.4 ft [1.04 m] (steep slopes or cliffs) and the data values cross to the next ambiguity interval.

## 2.2 TASK II: CONCEPTUAL DESIGN

The goal of Task II was to design a sensor to fulfill the requirements specified in Table 4. During the design, several basic issues were addressed, including wavelength selection, source and receiver optics, scan mechanism, and electronics.

In succeeding sections, each issue will be discussed followed by a brief examination of system performance. A summary of the ASV terrain sensor parameters concludes the conceptual design discussion.

### 2.2.1 Wavelength Selection

Selection of the most suitable wavelength was based on several considerations: covertness (0.7 to 14  $\mu\text{m}$ ), availability of sources and detectors, ease of implementation, size, power requirements, and eye safety. Based on covertness and the ready availability of sources and detectors, operation at either 0.82  $\mu\text{m}$  or 10.6  $\mu\text{m}$  were considered primary candidates. Millimeter sources were excluded because of the large aperture required to obtain the spatial resolution desired.

A comparison of the 0.82 and 10.6  $\mu\text{m}$  systems is presented in Table 5. The 0.82  $\mu\text{m}$  system is superior except for its ability to

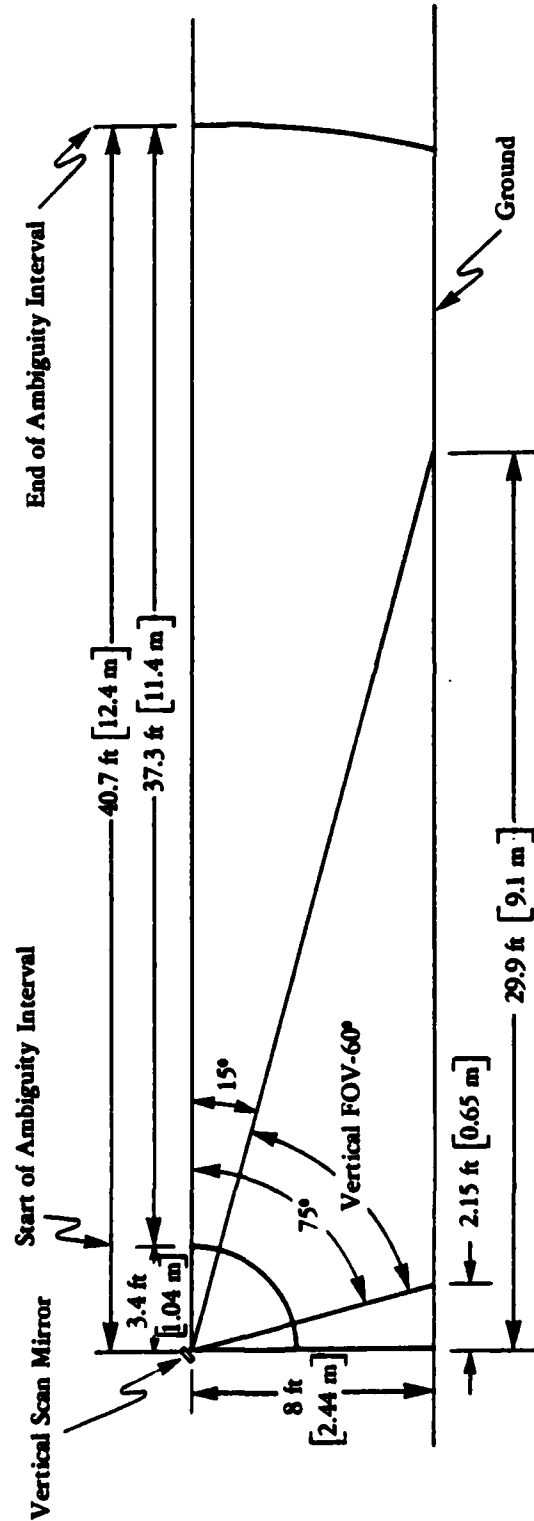
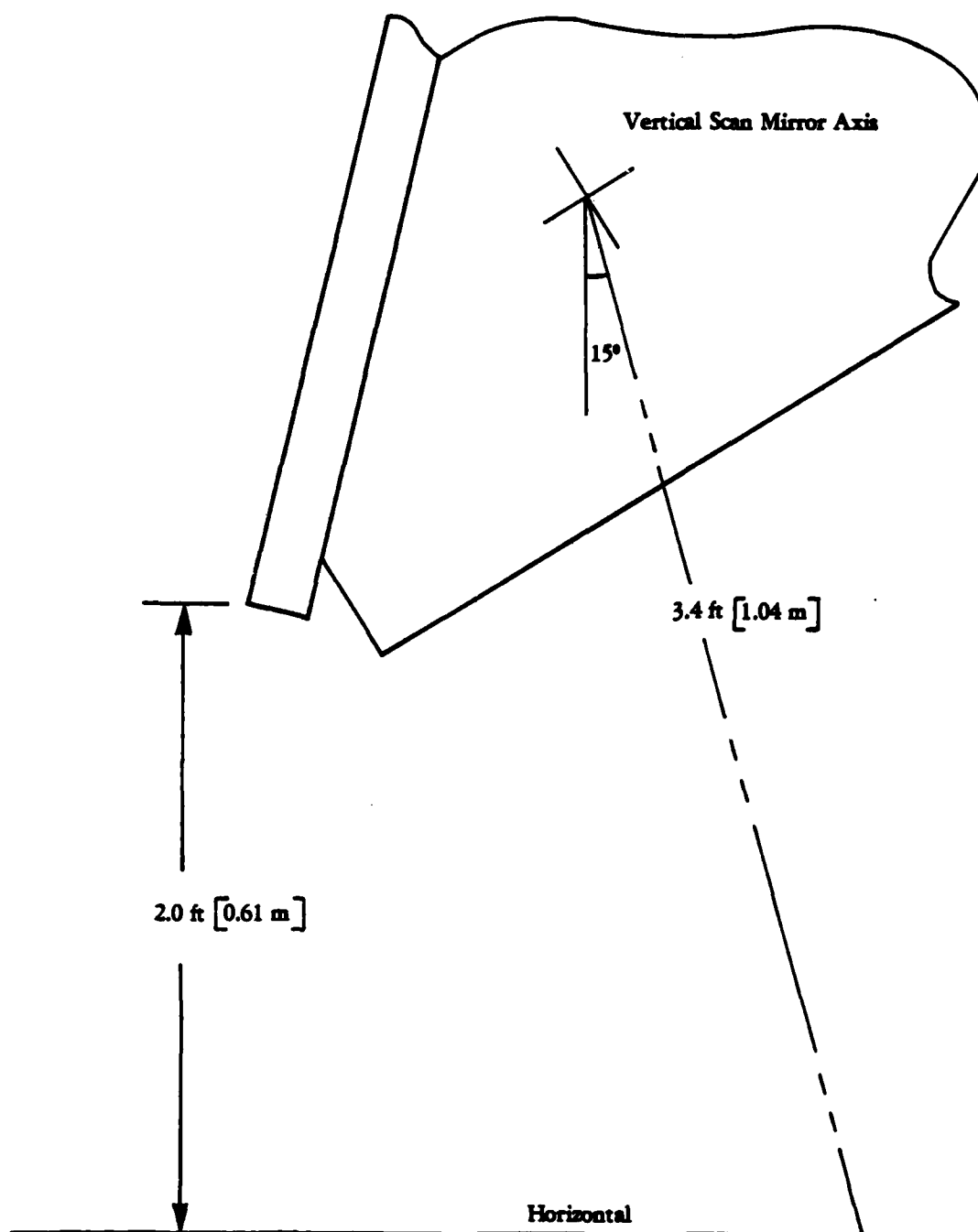


FIGURE 29. POSITION OF AMBIGUITY INTERVAL IN RELATION TO VERTICAL FOV



**FIGURE 30. SENSOR MEASUREMENT REFERENCE POINT**



TABLE 4. DESIGN GOALS

Spatial Resolution:	.5 x .5 ft (0.15 x 0.15 m) (X,Y) at 30 ft [9.14 m] range
TFOV:	60 deg vertical (15 to 75 deg depression angle) 60 deg horizontal $\pm 30$ deg from center line.
Frame Rate:	2 sec <sup>-1</sup>
Volume:	2 ft <sup>3</sup> [0.0566 m <sup>3</sup> ]
Weight:	50 lbs [23 Kg]
Power:	1 kW

penetrate fog or haze. In the ASV scenario, however, only short operational ranges (30 ft or 9.14 m) are of importance and, therefore, the increased penetrability of the longer wavelength is not significant. The higher reflectances for "natural" materials at 0.82  $\mu\text{m}$  compared to 10.6  $\mu\text{m}$  also favor the 0.82  $\mu\text{m}$  system.

TABLE 5. COMPARISON OF 0.82  $\mu\text{m}$  and 10.6  $\mu\text{m}$  SOURCES

	<u>0.82 <math>\mu\text{m}</math></u>	<u>10.6 <math>\mu\text{m}</math></u>
Source:	GaAs Laser Diode	CO <sub>2</sub> Laser
Source Size:	Very Small	Large 200 cm <sup>3</sup>
Modulation:	Internal	External 64 cm <sup>3</sup>
Detector:	Si APD	HgCdTe
	Uncooled	Cooled
SNR Limiting Factor:	Bright Sunlight	Detector Noise
Fog Haze Penetrability:	Fair (at short ranges)	Good
Safe Laser Exposure Times at 6 in. (15.2 cm) from scanner:	14 minutes	7 seconds

Laser eye safety exposure limits were calculated following the ANSI Z-136.1 standard. The distance from the horizontal scan mirror to the point of exposure was set at 6 in. [15.2 cm] which is inside the housing of the sensor. Laser power and beam size were 10 mW, 2.83 x 2.83 cm for 0.82  $\mu\text{m}$ , and 10 W, 2.83 x 2.83 cm for 10.6  $\mu\text{m}$ . The laser powers were derived from the signal-to-noise calculation. The

aperture was a compromise between the size of the scan mirrors, optics, and eye exposure power density. Scan geometry was identical for both cases. Using these parameters, the exposure time limit was calculated to be 13 min 50 sec for 0.82  $\mu\text{m}$  and 7 sec for 10.6  $\mu\text{m}$ .

Based on the advantages of size, temperature of operation, internal modulation, and eye safety, the 0.82  $\mu\text{m}$  system was selected as most appropriate to fulfill the requirements of the sensor. The 0.82  $\mu\text{m}$  system uses a GaAs laser diode source and a silicon avalanche photodiode (Si APD).

#### 2.2.2 Source and Receiver Optics

Source collimation and expansion optics are required on the laser diode to produce a 6 in. [15.2 cm] diameter beam at 30 ft (9.14 m). The divergence of the laser by itself would produce a much larger beam. If the laser diode selected does not have an integral collimation lens, two external cylindrical lenses could be used to collimate the beam. See Figure 31. A telescope expands the beam. Since the laser diode's emitting face is actually stripe shaped (i.e. long and narrow), the projected beam will be somewhat rectangular in shape.

A telescope similar to that used to expand the source serves as the receiver optics.

#### 2.2.3 Scan Mechanism

The scan mechanism consists of a rotating polygon mirror and a nodding mirror. See Figure 32. Galvanometers were considered but could not be used due to the size (and mass) of the mirrors required. See Table 6 and Figure 33. The frame rate and field of view to be scanned set the scan rate, which resulted in mirror angular accelerations in excess of 100,000 radians/sec<sup>2</sup>. The torque

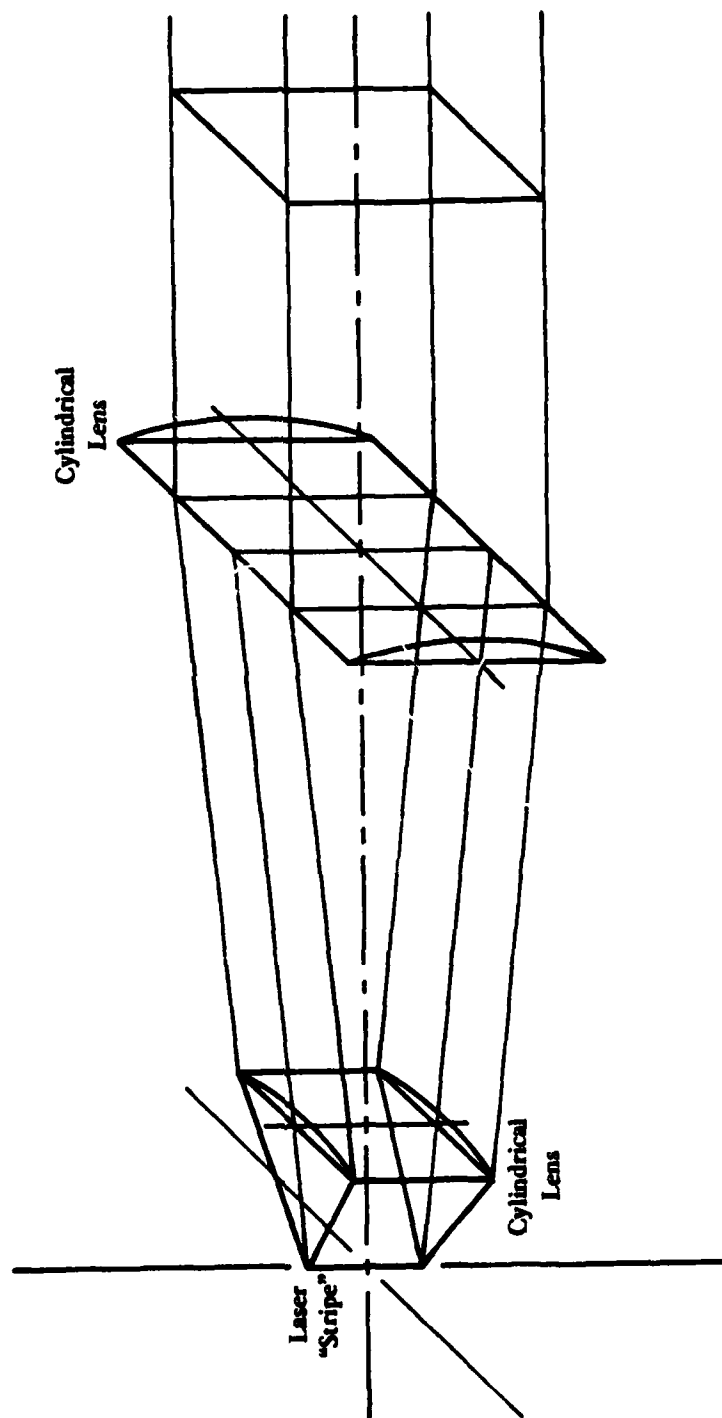


FIGURE 31. LASER COLLIMATION OPTICS

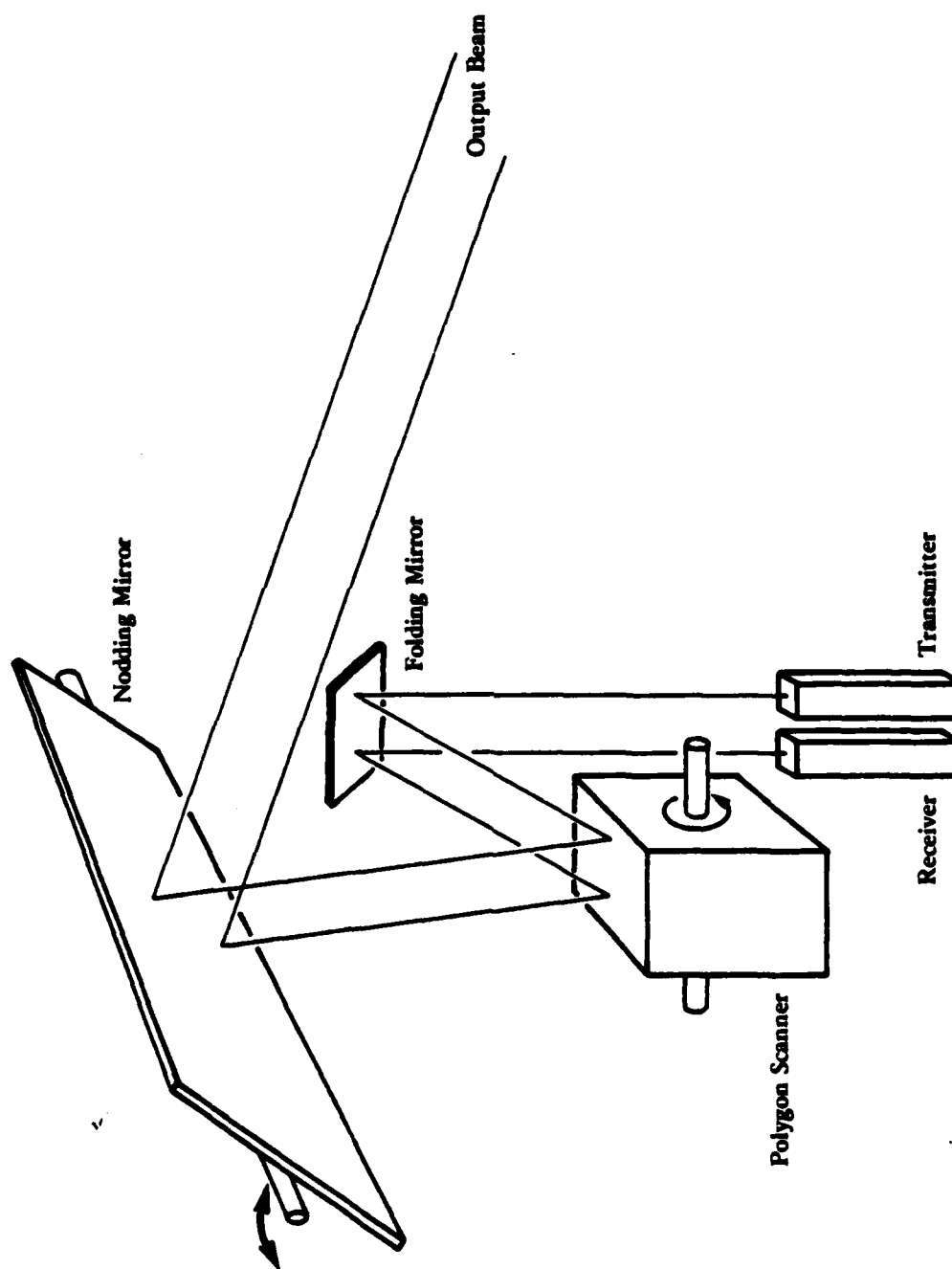


FIGURE 32. OPTICAL DIAGRAM OF SCANNER

TABLE 6. DRIVE REQUIREMENTS FOR AN OSCILLATING HORIZONTAL  
SCAN MIRROR (ACCELERATION)

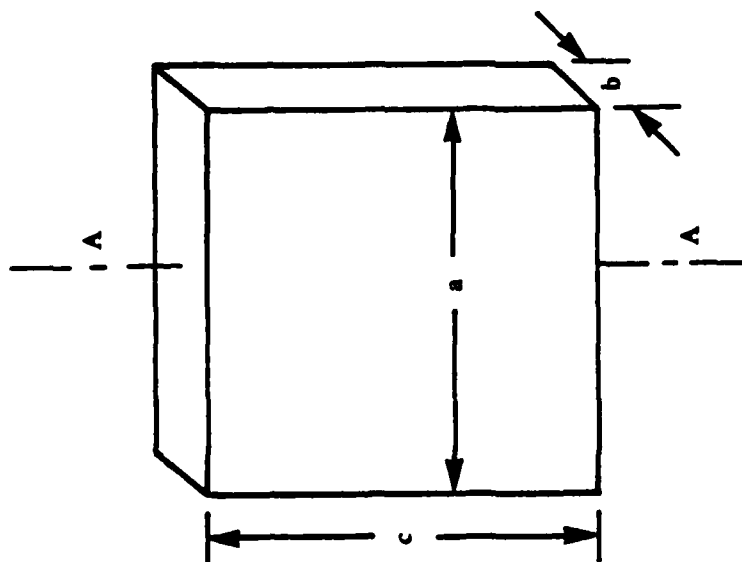
Scan Rate: 180 Lines Per Second

Scan Amplitude:  $\pi/2$  radians Peak To Peak

Mirror Angular Motion:  $\theta_n = \pi/8 \cos 2\pi 90t$

$$\ddot{\theta}_n = -(2\pi 90)^2 \pi/8 \cos 2/\pi 90t$$

Peak Angular Acceleration:  $(2\pi 90)^2 \pi/8 = 125,575 \text{ rad/sec}^2$



$$J_{AA} = \frac{1}{12} \frac{w}{g} (a^2 + b^2)$$

$$w = \rho a b c$$

$$a = c = 4.0 \text{ in.}$$

$$[10.16 \text{ cm}]$$

$$b = 5.0 \text{ in.}$$

$$[1.27 \text{ cm}]$$

$$\rho = 168 \text{ lb/ft}^3 \text{ (Aluminum)} [2.69 \times 10^3 \text{ kg/m}^3]$$

$$J_{AA} = \frac{1}{12} \frac{(168)(4)(4)(5)}{(32.17)(1728)} \left[ \left( \frac{4}{12} \right)^2 + \left( \frac{5}{12} \right)^2 \right]$$

$$= 2.27 \times 10^{-4} \text{ lb ft sec}^2/\text{rad}$$

$$[3.143 \times 10^{-4} \text{ N} \cdot \text{m sec}^2/\text{rad}]$$

$$\text{Peak Torque} = J_{AA} (2\pi 90)^2 \frac{\pi}{8}$$

$$= 28.551 \text{ lb ft}$$

$$[3.947 \text{ N} \cdot \text{m}]$$

FIGURE 33. DRIVE REQUIREMENTS FOR AN OSCILLATING HORIZONTAL SCAN MIRROR (TORQUE).

Since the oscillating assembly includes the shaft and drive motor rotor, the polar moment of inertia for the assembly would be much greater than  $J_{AA}$ . Then, the peak torque requirement would be much greater than 30 lb ft [4.14 N · m].

requirements to make the mirror move at these accelerations are in excess of 28 lb ft [3.947 N.m]. The rotating polygon is four-sided and is motor-driven at a constant rate requiring .122 lb-ft [0.017 N.m.] of torque. The nodding mirror is servo driven. The entire package, Figure 34, measures (H x W x D): 12 x 12.5 x 5 in [25.4 x 31.7 x 12.7 cm], less motor and servo. Increasing the TFOV of the scanner greatly increases the size of the mirrors, Figure 35. For example, for a TFOV (EL x AZ) of 90 x 90 deg the nodding mirror measures (H x W): 7.25 x 18.5 in. [18.4 x 47 cm]. While a large TFOV is possible, the size, weight, and required mirror drive power are excessive when compared to the power available.

The scanner will generate a left-to-right, bottom-to-top scan pattern much like a television raster scan. The modified raster scan was arrived at through discussions between Battelle, OSU, and ERIM, all of whom are participants in the parameter identification for the terrain sensor for the 1984 ASV.

The scanner ground TFOV is shown in Figure 36. This figure is based on a TFOV of 60 x 60 deg and a scanner height of 8 ft [2.44 m] above ground level. Figure 37 illustrates the overlap of these TFOVs based on a vehicle velocity of 10 ft/sec [3.05 m/s]. Six frames of data are available on a corridor  $\pm 6$  ft [ $\pm 1.83$  m] from the centerline of the vehicle.

#### 2.2.4 Electronics

A block diagram of the signal processing electronics is shown in Figure 38. A block diagram of the digital phase detector is presented in Figure 39. The light reflected from the scene illuminates the detector which converts the optical signal from the preamp. The filters then select the desired spectral portion of the signal from the detector. Prior to the limiter, the amplitude signal is picked off and made available to generate a conventional reflectance image of



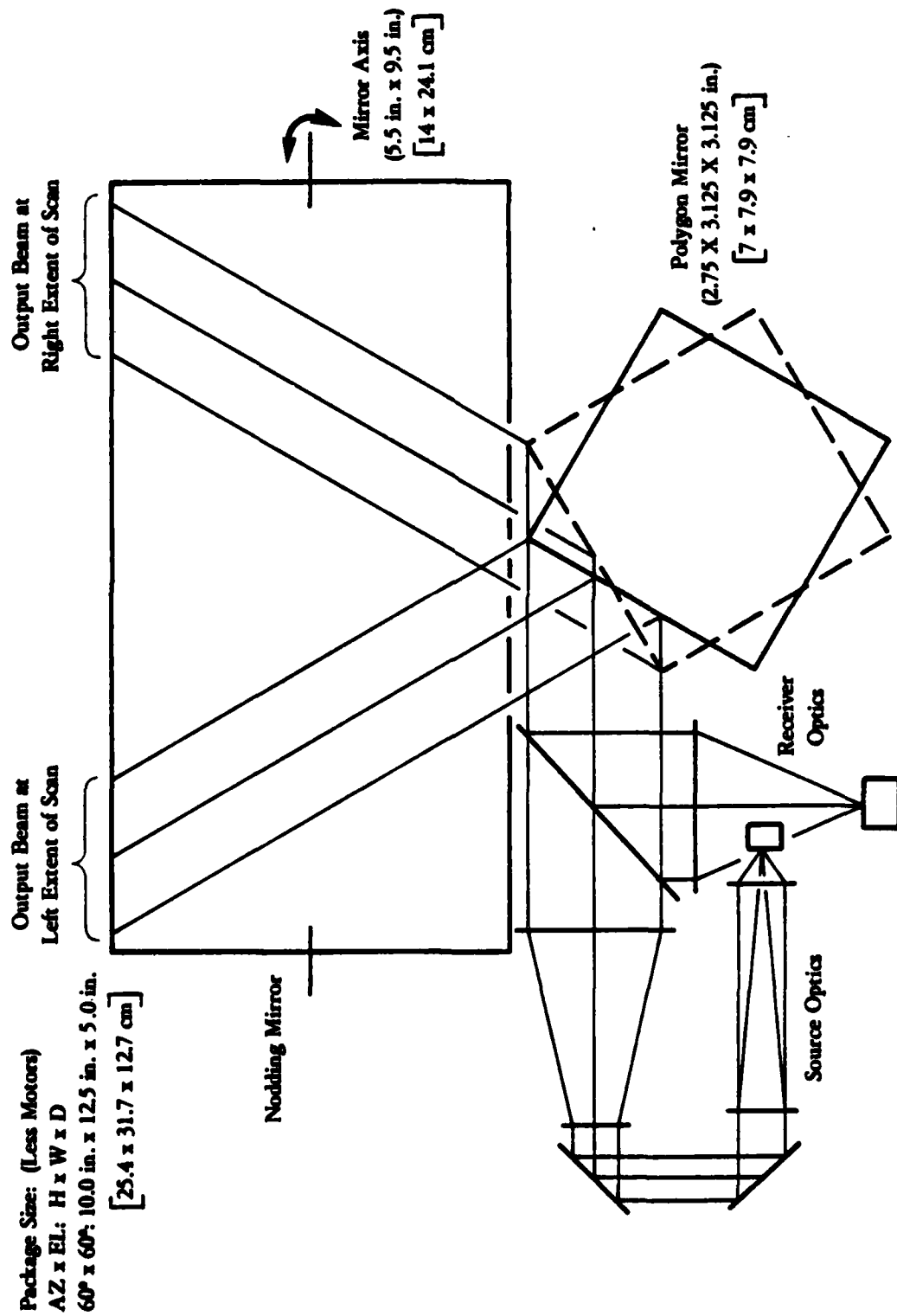


FIGURE 34. REPRESENTATION OF 60° x 60° SCAN SYSTEM

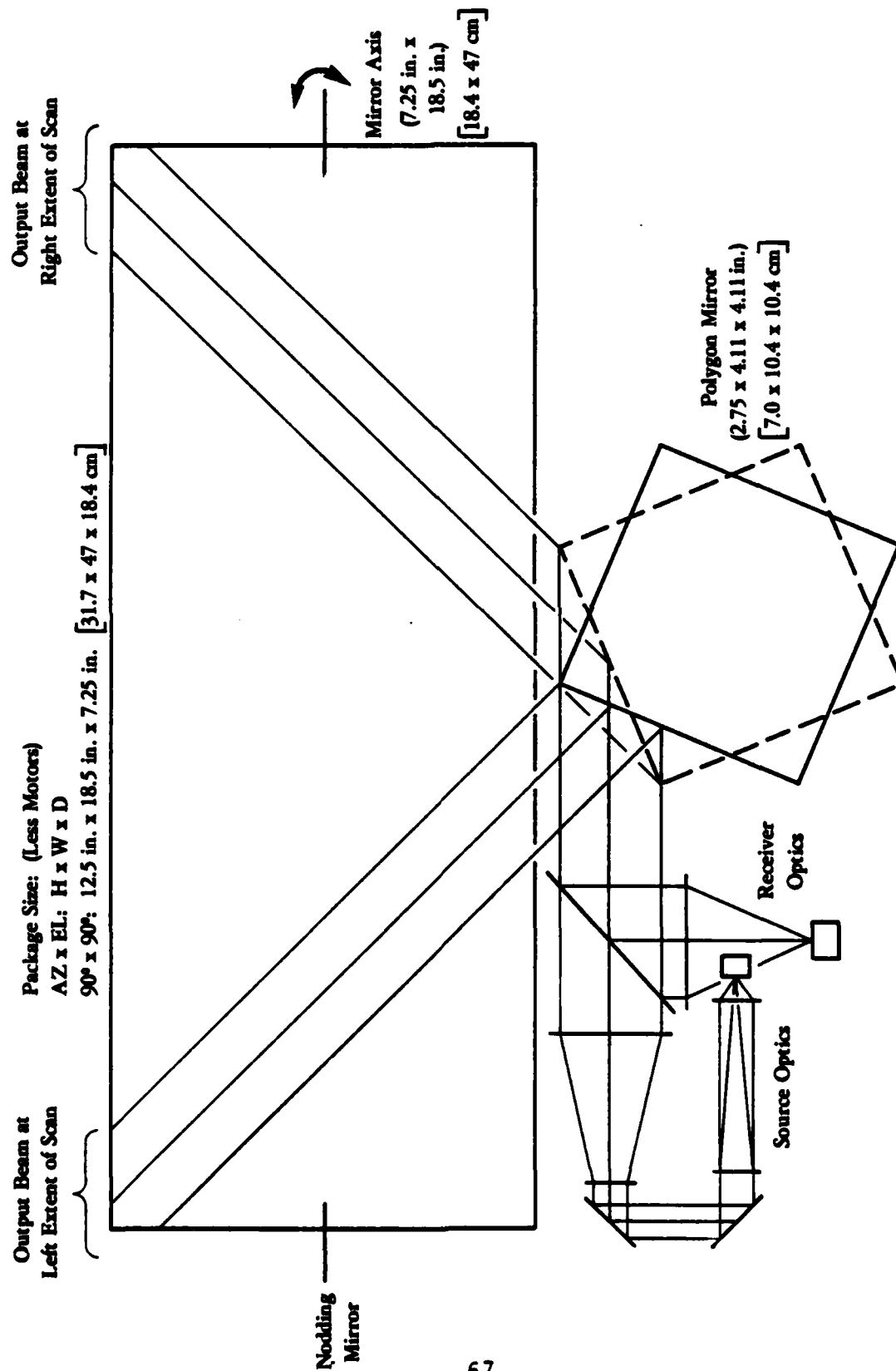


FIGURE 35. SCALE REPRESENTATION OF 90° x 90° SCAN SYSTEM

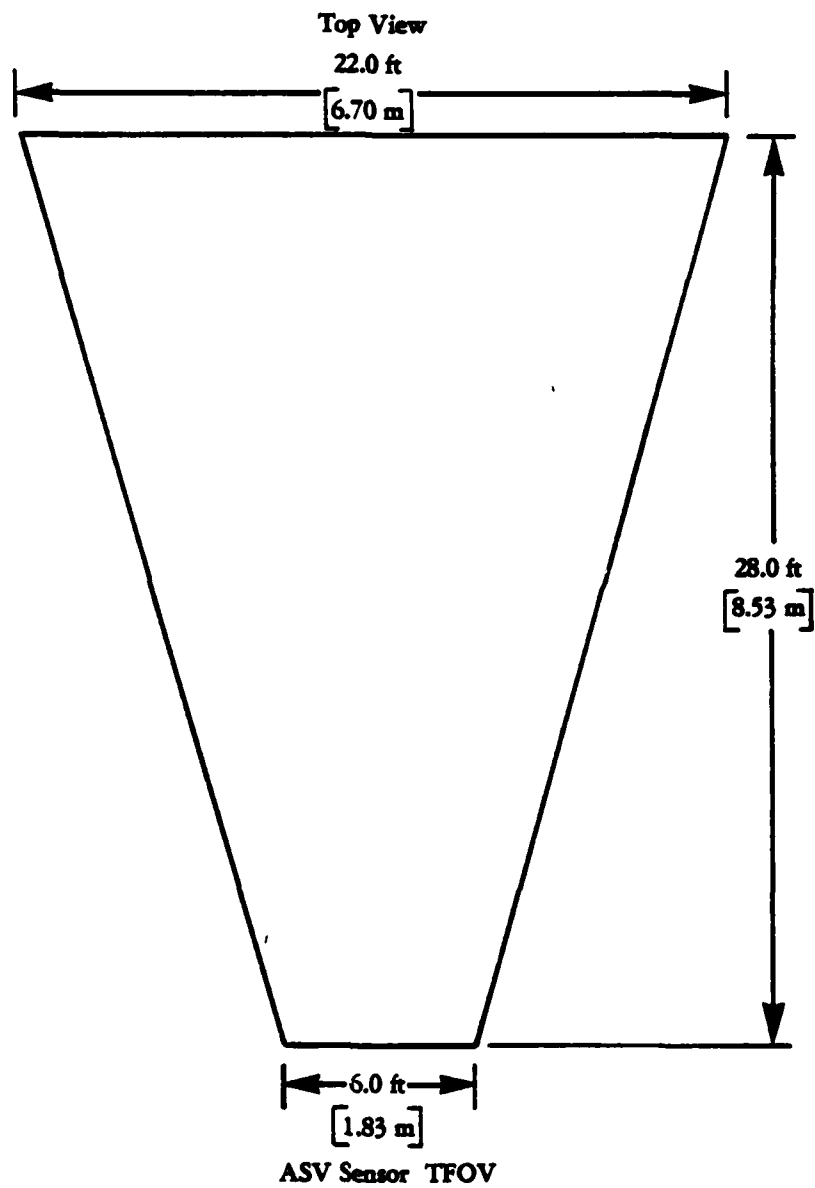


FIGURE 36. ASV SENSOR FIELD OF VIEW

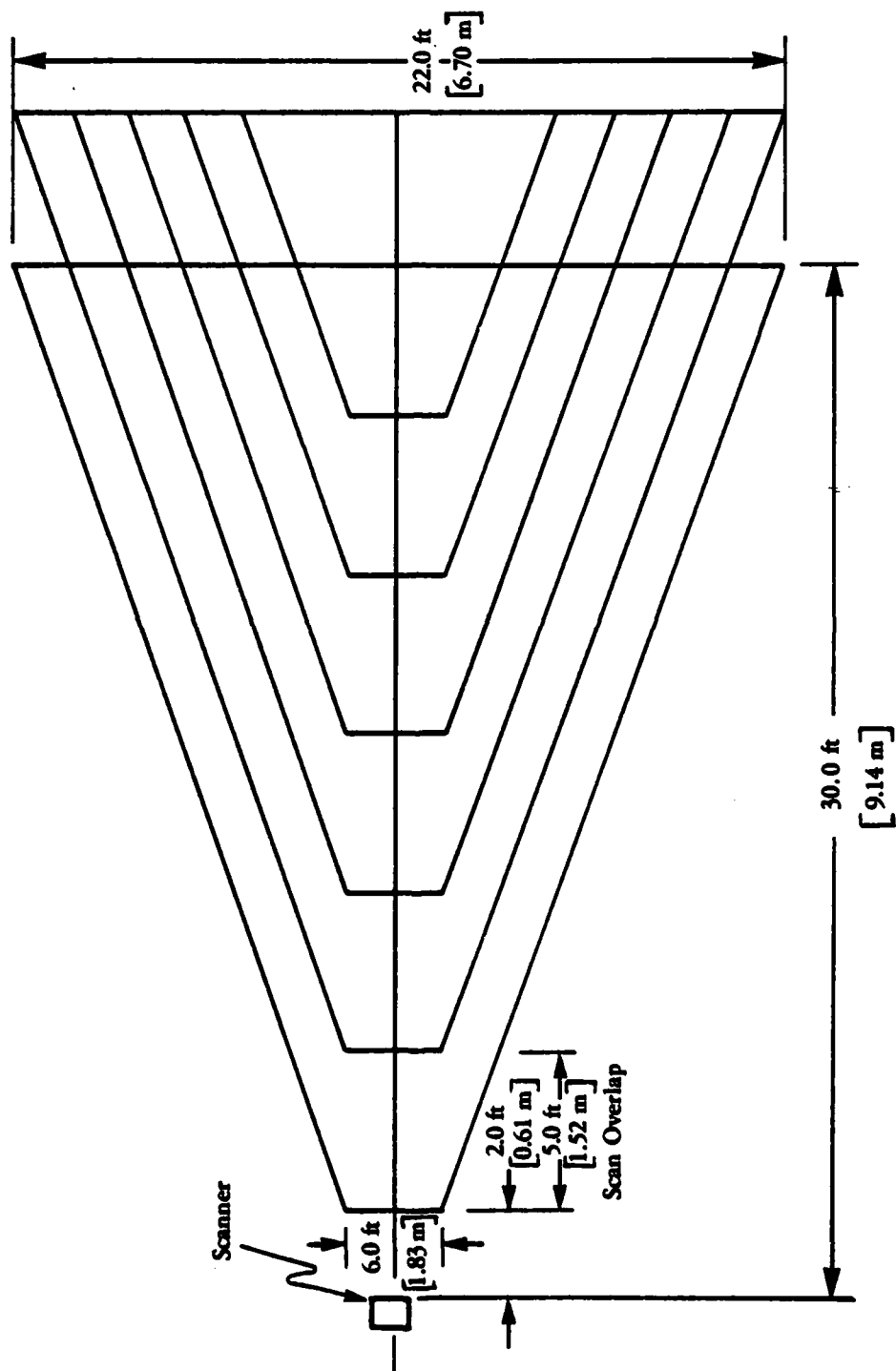


FIGURE 37. SCAN GEOMETRY (TOP VIEW 10 ft/sec)

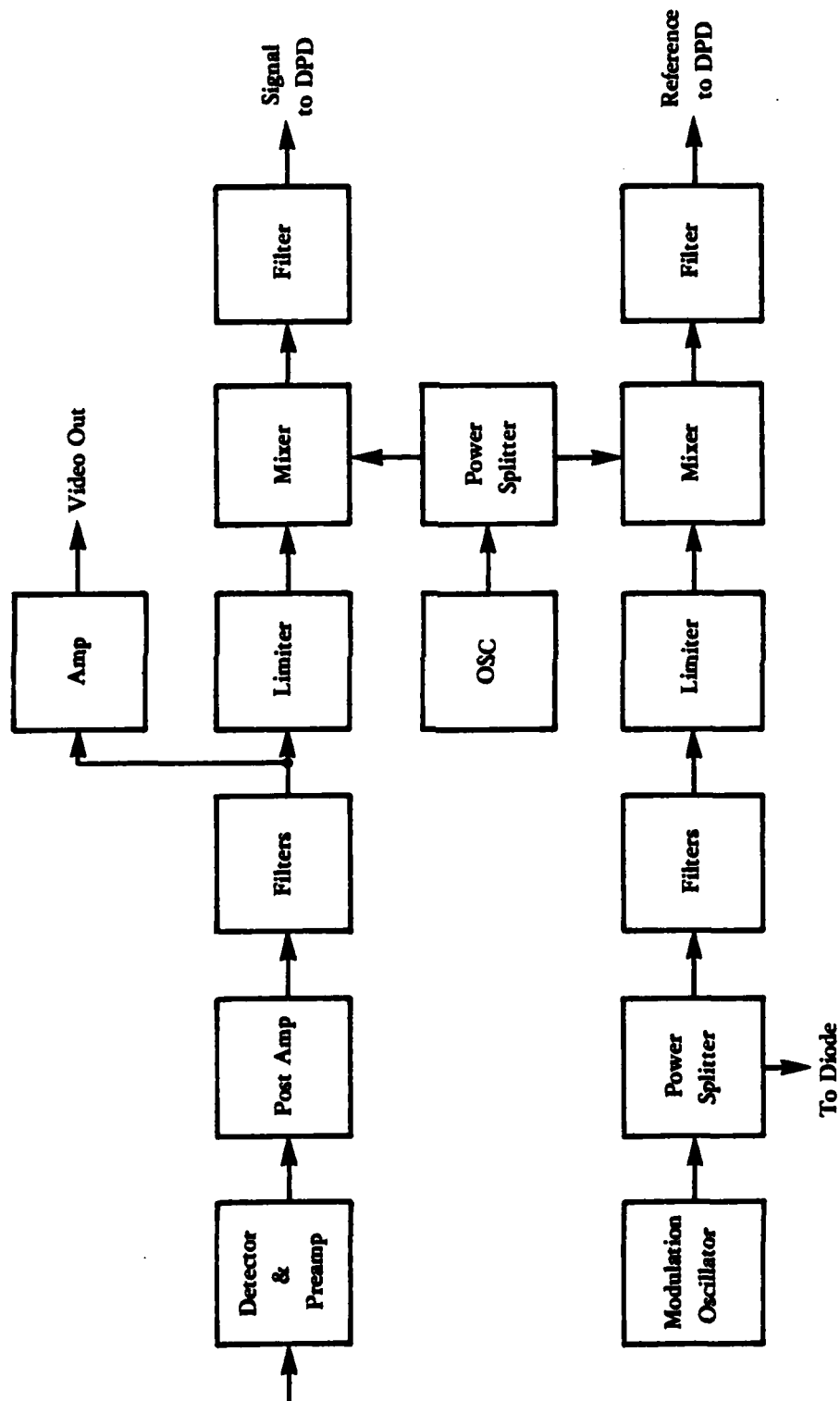


FIGURE 38. SIGNAL PROCESSING ELECTRONICS BLOCK DIAGRAM

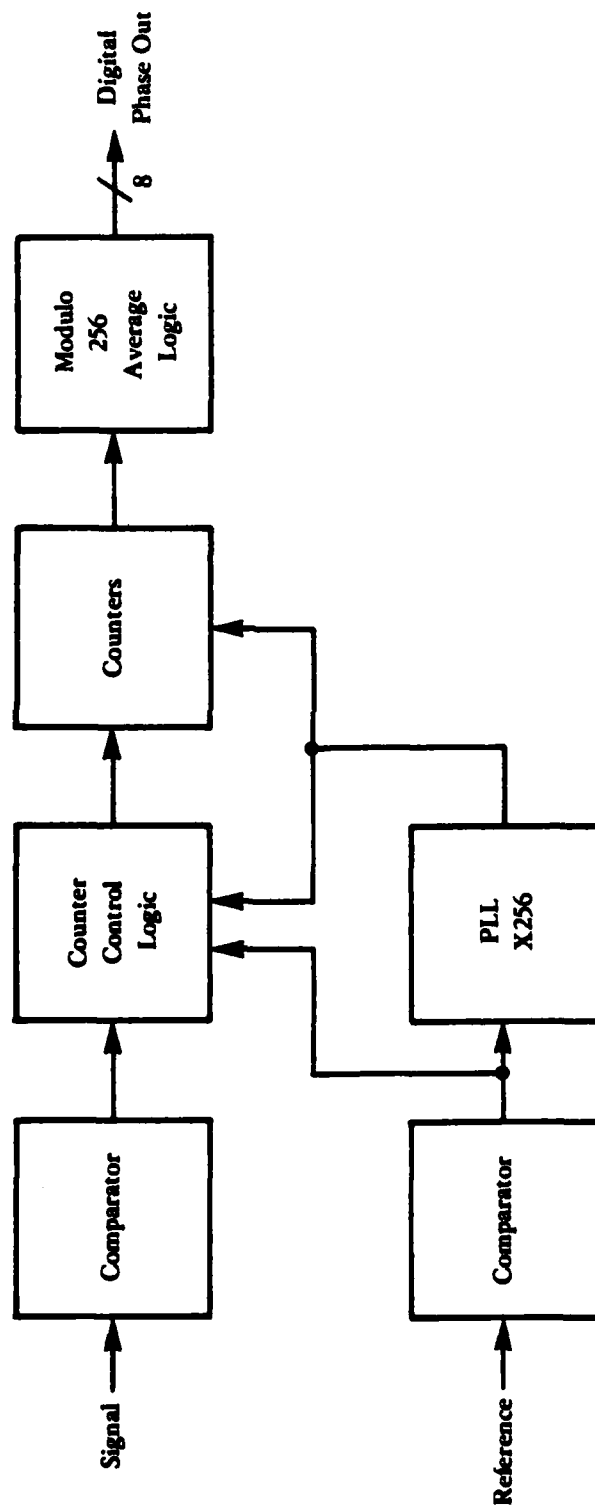


FIGURE 39. DIGITAL PHASE DETECTOR BLOCK DIAGRAM

the scene. The limiters remove any amplitude information leaving only the phase information which measures the range. The mixer acts as a frequency translator and changes the frequency of the range signal while preserving the phase information. The filters remove unwanted products of the frequency translation.

A similar path is followed in the reference channel where the signal source is the modulation oscillator instead of the detector.

The signals output from the signal processing electronics go to the digital phase detector shown in Figure 39. The digital phase detector (DPD) consists of a pair of comparators, a phase-locked loop (PLL) frequency multiplier, a control logic, and counters. The comparators convert the input signals to logic levels. The reference signal frequency is then multiplied by 256 to generate a high speed clock that drives the counters. The logic control starts the counter on a leading edge of the reference signal and stops it on the leading edge of the information signal. The count is thus a measure of the phase difference between the reference and information signal lines. The output is an 8-bit digital word which is the range to the scene.

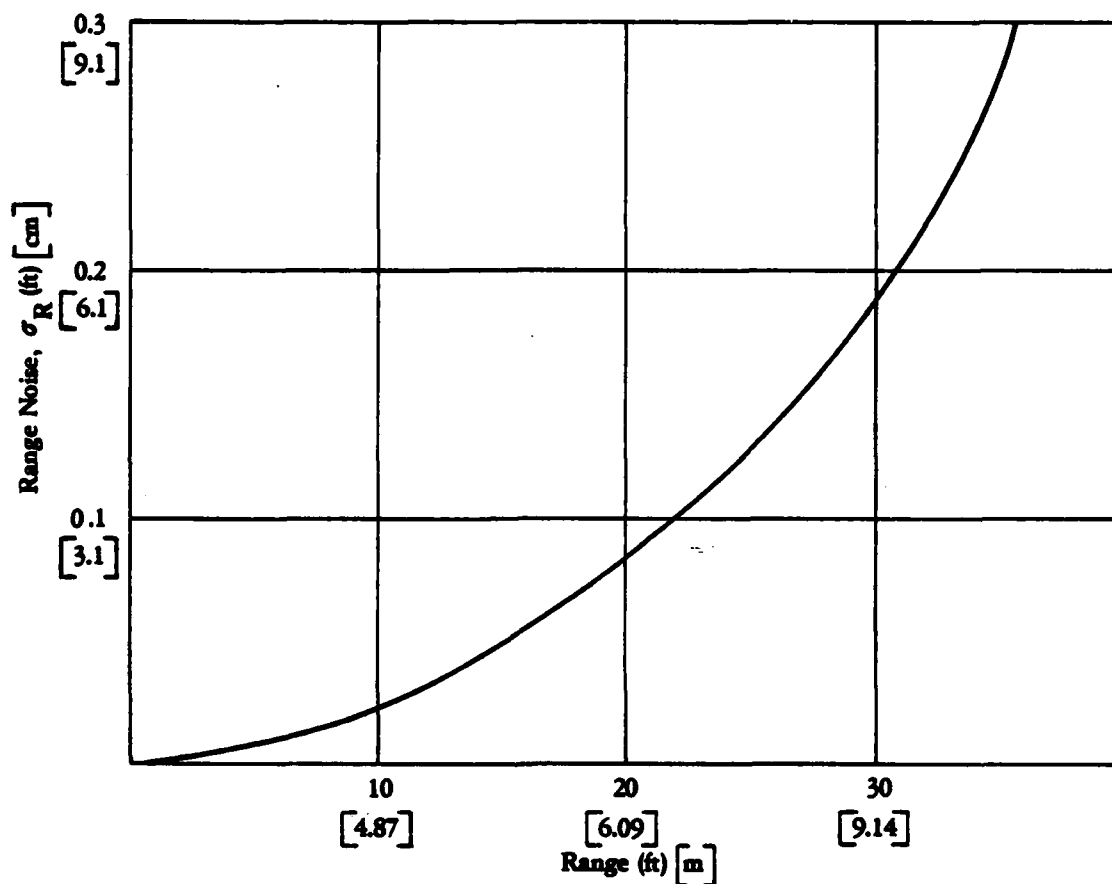
Specifications for the electronics are:

- 65 dB dynamic range with less than 5° phase shift
- 16 kHz bandwidth (32 kHz sampling rate)
- Digital phase detector: 8-bit resolution

The dynamic range is achievable with commercially available components. The bandwidth is set by the frame rate and FOV, while the phase detector resolution comes mainly from the convenience of having data in a byte or 8-bit format.

#### 2.2.5 System Performance

System performance is summarized in Figures 40 and 41. Figure 40 illustrates the system range noise versus range to the object. It can



Range Noise vs. Range for:

$\rho$  = Scene Reflectivity = 0.3

$\langle P_L \rangle$  = Average Laser Power = 0.02 W

$A_r$  = Receiver Area = 4.0 cm<sup>2</sup>

$\tau$  = Total Transmit/Receive Path Transmission = 0.39

$B$  = Noise Bandwidth = 100 kHz

$\Delta\lambda$  = Optical Filter Bandwidth = 0.05  $\mu$ m

$\Delta r$  = Ambiguity Interval = 30.0 ft [9.14 m]

Receiver IFOV = 1°

Detector = RCA APD

FIGURE 40. RANGE NOISE VS. RANGE



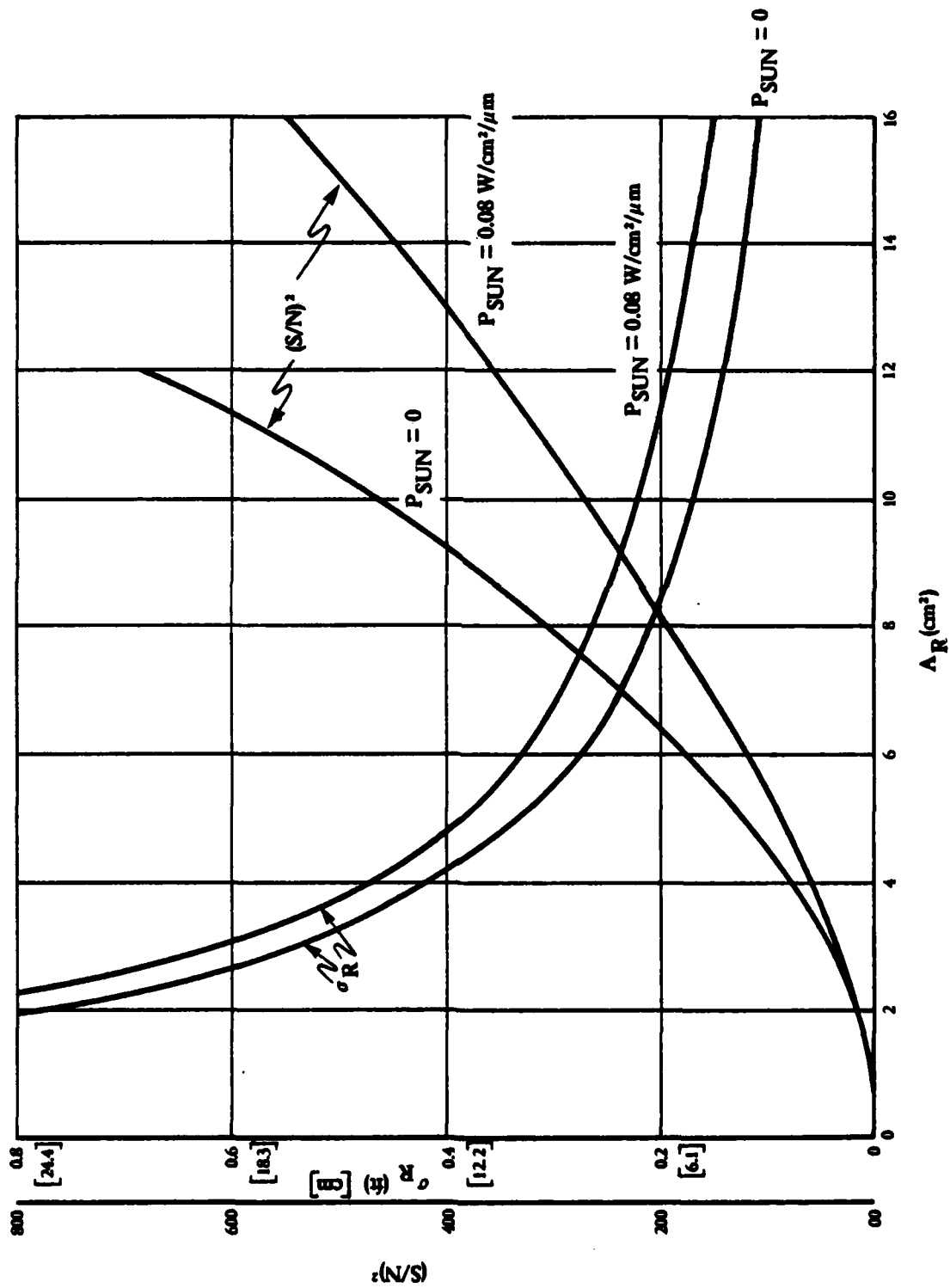


FIGURE 41. RANGE NOISE AND S/N VS. RECEIVER APERTURE

be seen that at 30 ft [9.14 m] the noise is 2 in. [5.08 cm], at 8 ft [2.44 m] it is 0.2 in. [0.51 cm]. The improvement in range noise rate (S/N) comes with shorter sensor-to-object range.

Figure 41 illustrates the system S/N ratio and the system range noise versus a given receiver aperture for the cases of bright sunlight and night operation. The system operates better at night than in the daylight due to the absence of background illumination. The S/N improves as the aperture is increased. While further improvement of the S/N ratio can be obtained by increasing the aperture size, a severe penalty is incurred since increases in aperture result in increases in the size and mass of the rotating and nodding mirrors and associated optics. There is a limit as to how large (massive) these mirrors can be and still move them at the required rates. The receiver area arrived at for the proposed design is (4.0 cm<sup>2</sup>) which yields a S/N ratio of 18 dB.

The equation used to derive the S/N is presented below. The equation is derived for a power signal-to-noise. The term that makes up the left portion of the denominator is the shot noise term while the right portion is the background noise of the detector and preamplifier.

An example calculation of system S/N is presented. Ambient illumination and range have been placed at their maximum to ensure a worst case situation.

$$(S/N)^2 = \frac{\langle i^2 \rangle_{sig}}{\langle i^2 \rangle_{noise}} = \frac{2S(w) \left[ \frac{\rho}{\pi} \langle P_L \rangle \tau \frac{A_R}{R^2} \dot{R} \right]^2}{2e \left[ \frac{\rho}{\pi} \langle P_L \rangle \tau \frac{A_R}{R^2} \dot{R} + \frac{\rho}{\pi} p_{sun} \tau \frac{A_R}{R^2} \Delta \lambda A_f \dot{R} \right] FB + (NEP)^2 R^2 B}$$

- where
- $S(w)$  = modulation coefficient,  
(for sinusoidal modulation  $S(w) = .25$ )
  - $\rho$  = reflectivity of the scene = .3
  - $\langle P_L \rangle$  = average laser power = .02 W
  - $\tau$  = transmittance of receiver and transmitter optics  
and 2 way atmosphere = .39
  - $A_R$  = area of receiver = 4 cm<sup>2</sup>
  - $R$  = range to object = 30 ft [9.14 m]
  - $\dot{R}$  = responsivity of detector = .55 A/W
  - $e$  = charge of an electron =  $1.6 \times 10^{-19}$  coulomb
  - $P_{\text{sun}}$  = sun illumination on a bright day at the equator  
at .8  $\mu\text{m}$  = .08 W/cm<sup>2</sup>/ $\mu\text{m}$
  - $\tau'$  = transmittance of receiver optics and 1 way  
through atmosphere = .6
  - $\Delta\lambda$  = optical filter bandwidth = .05  $\mu\text{m}$
  - $A_f$  = area of receiver instantaneous field-of-view  
(IFOV) on ground = 200 cm<sup>2</sup> for .5 ft dia circular  
area
  - $F$  = avalanche excess noise factor = 2.06
  - $B$  = bandwidth =  $10^5$  Hz
  - NEP = noise equivalent power =  $1.64 \times 10^{-13}$  W/Hz<sup>1/2</sup>

Substituting into the equation above:

$$(S/N) = \frac{1.92 \times 10^{-18}}{4.66 \times 10^{-21} + 8.10 \times 10^{-22}} = 321$$

When the  $(S/N)^2$  is greater than 30 one can relate  $(S/N)^2$  and  $\sigma_R$ , the standard deviation in range due to noise, by the equation

$$\frac{\sigma_R}{\Delta R} = \frac{1}{2\pi} \frac{1}{\sqrt{2(S/N)^2}} = 6 \times 10^{-3} \text{ or } .6\%$$

( $\Delta R$  = ambiguity interval)

where  $\sigma_R$  = 0.6% of the ambiguity interval, or for the case where  $\sigma_R$  = 30 ft (9.14 m),  $\sigma_R$  = 2 in. [5.08 cm].

#### 2.2.6 ASV Terrain Sensor Parameters

Based on the performance requirements of the sensor and the conceptual design study, the sensor parameters listed in Table 7 have been defined.

TABLE 7. SENSOR PARAMETERS

IFOV:	1 deg; footprint of 0.5 ft (15.2 cm) at 32 ft [9.75 m], and 0.14 ft [4.27 cm] at 8 ft [2.44 m]
Sample Rate:	32 kHz
Frame Rate:	2 per second
Scan Range:	Vertical 60 deg, 15 deg to 75 deg depression angle; Horizontal 60 deg, $\pm 30$ deg from center line
Range Resolution:	8 bits, 1 bit = 0.125 ft [3.81 cm]
Range Noise:	0.2 ft [6.10 cm] at 32 ft [9.75 cm] reflectance = 10%, bright sunlight
Ambiguity Interval:	32 ft (9.7 m)
Scanner Output Format:	$\theta$ , $\phi$ , Range
Wavelength:	.82 $\mu\text{m}$
Volume:	2 ft <sup>3</sup> [0.566 m <sup>3</sup> ]
Weight:	50 lb
Power:	480 W
Power Interface:	24V, 20 Ampers
Data Interface:	Byte Parallel

### SECTION 3

#### CONCLUSIONS AND RECOMMENDATIONS

Early discussions on the characteristics of the ASV terrain sensor concluded that a 3D terrain sensor could be of considerable assistance in improving the performance of the ASV. The ability of the sensor to generate a 3D picture of the terrain, especially mountainous terrain, could not be matched by other vision systems. The ASV sensor is not infallible; for example, it cannot see through deep snow to indicate where adequate footing might be found, but then no vision system can do this. Other problems were discussed, but ASV program participants concurred that a 3D vision system would enhance ASV performance.

The results of the design study have led to the definition of the sensor parameters, given in Table 7. These parameters have been coordinated with DARPA, OSU, and Battelle and have been tailored to the special characteristics of the ASV.

The 0.82  $\mu\text{m}$  wavelength system fulfills the need for a light-weight, compact, and energy efficient system. The design is feasible with available technology and provides a high degree of safety to personnel. Range and position data output from the sensor are directly available to onboard processors without the need for preprocessing as in a stereo system where images must be matched and the range determined by a triangulation calculation. In short, the sensor fulfills all the requirements set down for an ASV terrain sensor.

It is recommended that the sensor design be accepted to fulfill ASV vision requirements.